



Deposited via The University of Leeds.

White Rose Research Online URL for this paper:

<https://eprints.whiterose.ac.uk/id/eprint/136495/>

Version: Accepted Version

Article:

Krop, EM, Hetherington, MM, Holmes, M et al. (2019) On relating rheology and oral tribology to sensory properties in hydrogels. *Food Hydrocolloids*, 88. pp. 101-113. ISSN: 0268-005X

<https://doi.org/10.1016/j.foodhyd.2018.09.040>

© 2018, Elsevier. Licensed under the Creative Commons Attribution-NonCommercial-NoDerivatives 4.0 International <http://creativecommons.org/licenses/by-nc-nd/4.0/>

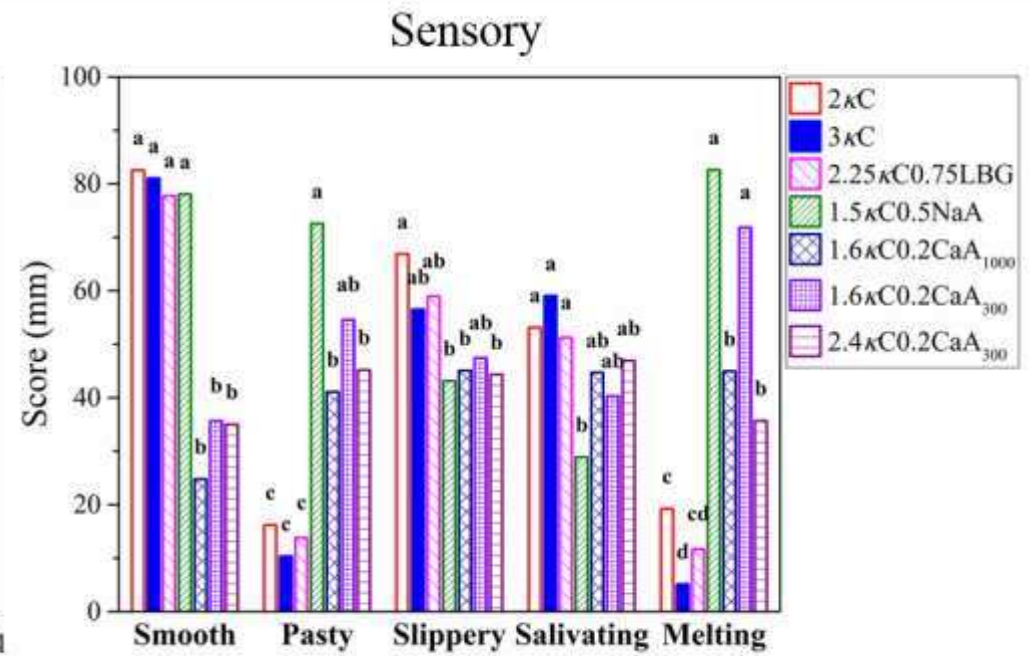
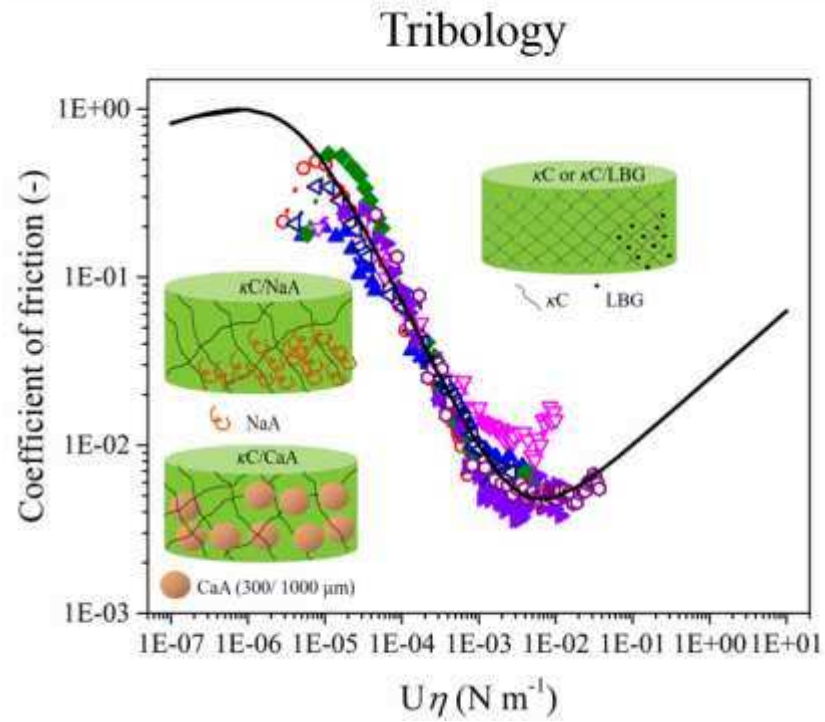
Reuse

This article is distributed under the terms of the Creative Commons Attribution-NonCommercial-NoDerivs (CC BY-NC-ND) licence. This licence only allows you to download this work and share it with others as long as you credit the authors, but you can't change the article in any way or use it commercially. More information and the full terms of the licence here: <https://creativecommons.org/licenses/>

Takedown

If you consider content in White Rose Research Online to be in breach of UK law, please notify us by emailing eprints@whiterose.ac.uk including the URL of the record and the reason for the withdrawal request.

Graphical Abstract



Highlights

- Oral processing of hydrogels was influenced by introducing structural inhomogeneity
- Correlations existed between chewing attributes and gel fracture, boli rheology
- Friction coefficient (μ) corroborated Stribeck master curve only in mixed regime
- 'Pasty' was inversely correlated with μ of bolus filtrate at orally relevant speed
- 'Salivating' correlated with initial fracture properties, boli rheology and tribology

1 **On relating rheology and oral tribology to sensory**
2 **properties in hydrogels**

3

4 *Emma M. Krop^a, Marion M. Hetherington^b, Melvin Holmes^a, Sophie Miquel^c, Anwesh*
5 *Sarkar^{a*}*

6

7 ^a Food Colloids and Processing Group, School of Food Science and Nutrition, University of Leeds,
8 Leeds LS2 9JT, United Kingdom

9 ^b School of Psychology, University of Leeds, Leeds LS2 9JT, United Kingdom

10 ^c Mars Wrigley Confectionery, 1132 West Blackhawk Street, Chicago, IL 60642, USA

11

12

13

14

15

16

17

18

19 *Corresponding author:

20 Dr Anwesh Sarkar

21 Food Colloids and Processing Group,

22 School of Food Science and Nutrition, University of Leeds, Leeds LS2 9JT, UK

23 E-mail address: A.Sarkar@leeds.ac.uk

24 Phone: +44 (0) 113 343 2748

25 Abstract

26 The aim of this study was to understand the relationship between rheological, tribological and
27 sensory properties (n=11 panellists) of hydrogels differing in hydrocolloid type, concentration
28 and degree of inhomogeneity. Fracture properties of hydrogels containing different ratios of κ -
29 carrageenan (κ C) and/or locust bean gum (LBG), sodium alginate (NaA), 300/1000 μ m calcium
30 alginate beads (CaA) at 1-4 wt% concentration were determined. Viscosity and friction
31 coefficients (μ) of the hydrogel-boli after simulated oral processing were characterized.
32 Tribology measurements were conducted in a polydimethylsiloxane ball/disc set-up with pre-
33 adsorbed artificial salivary film at 37 °C. 'Scaling' with boli viscosity showed good agreement
34 of observed data with the Stribeck master curve, however only in the mixed regime *i.e.* at
35 intermediate values of the product of velocity and lubricant viscosity ($U\eta$). Low μ values of
36 gel boli in the boundary regime were largely driven by the formation of a viscous layer of bolus
37 fragments between opposing surfaces. Fracture properties of hydrogels and boli viscosity were
38 correlated with all chewing-related texture attributes *i.e.* 'firm', 'elastic', 'chewy' and
39 'cohesive' and inversely correlated with lubrication-related attributes 'melting' and 'pasty'
40 ($p < 0.05$). On the other hand, μ of the bolus filtrate at orally relevant speeds (50 mm/s) was
41 inversely correlated with lubrication-related attributes 'pasty' and positively with 'slippery'
42 ($p < 0.05$). The lack of correlations with 'smooth' could be explained due to sample
43 inhomogeneity and the absence of 'ball-bearing'-ability of the gel beads. A combination of
44 initial fracture properties, boli viscosity and tribology of bolus filtrates (mixed regime)
45 impacted the lubrication-related attribute 'salivating' ($p < 0.05$).

46

47 Keywords

48 Oral processing; Sensory attributes; Texture; Bolus viscosity; Oral Tribology; Lubrication

49 **1. Introduction**

50 Oral processing strategies, such as higher number of chews and longer oral residence time have
51 recently been linked to lower self-reported hunger and food intake in controlled experiments
52 (Krop, et al., 2018; Miquel-Kergoat, Azais-Braesco, Burton-Freeman, & Hetherington, 2015).
53 Hence, there has been a gradual increase in research efforts to understand and alter oral
54 processing *i.e.* in-mouth chewing and lubrication by means of microstructural engineering
55 (Laguna, Hetherington, Chen, Artigas, & Sarkar, 2016; Laguna & Sarkar, 2016).
56 Understanding the characteristics of oral processing (chewing, lubrication) has drawn
57 significant research attention with the focal point recently shifting from rheology to tribology.
58 This is largely due to the current consensus on the transformation during oral processing from
59 rheology (bulk property) to tribology (surface property of food-saliva bolus based lubricants)
60 (Chen & Stokes, 2012; Garrec & Norton, 2013; Laguna & Sarkar, 2017; Pradal & Stokes, 2016;
61 Prakash, Tan, & Chen, 2013; Sarkar, Kanti, Gulotta, Murray, & Zhang, 2017a; Stokes, Boehm,
62 & Baier, 2013; van Stee, de Hoog, & van de Velde, 2017).

63 An important aspect of oral processing of solid and semi-solid foods is the incorporation
64 of saliva to form a swallowable food bolus. Saliva is a complex biological fluid that consists
65 of mainly water (~99.5%), various enzymes (α -amylase, lysozyme) and proteins, (~0.3%),
66 small organic compounds and inorganic salts (Sarkar, Goh, & Singh, 2009; Sarkar & Singh,
67 2012; Sarkar, Ye, & Singh, 2017b). The key protein component in human saliva is highly
68 glycosylated mucin, which mainly contributes to the lubrication and shear-thinning properties
69 of saliva (Schipper, Silletti, & Vingerhoeds, 2007; Vijay, Inui, Dodds, Proctor, & Carpenter,
70 2015). The incorporation of saliva over time within a single bite episode has a major effect on
71 the texture perception (Funami, Ishihara, Nakauma, Kohyama, & Nishinari, 2012; Hutchings
72 & Lillford, 1988). The in-mouth friction properties might change significantly due to the
73 interactions between food and salivary components, such as mucins and salts. However, few

74 studies have used real human saliva, or artificial saliva formulation, within *in vitro* oral
75 processing experiments to understand its impact on the mechanical properties, such as viscosity
76 or friction coefficient, and correlated such data to sensory perception (Laguna, Farrell, Bryant,
77 Morina, & Sarkar, 2017a; Laguna, et al., 2017b; Morell, Chen, & Fiszman, 2017).

78 This study creates a unique body of evidence on the initial fracture properties of
79 hydrogels, viscosity and tribology of hydrogel boli created using simulated oral processing
80 (using artificial saliva formulation) and sensory profiling (descriptive analysis) to understand
81 the relationship between mechanical and sensory properties. To investigate food oral
82 processing, biopolymeric ‘hydrogels’ have been the choice as model solids and semi-solid
83 foods in literature (Hayakawa, et al., 2014; Hori, et al., 2015; Kohyama, et al., 2015; Laguna,
84 et al., 2016; Laguna & Sarkar, 2016; Santagiuliana, Piqueras-Fiszman, van der Linden, Stieger,
85 & Scholten, 2018). This is because hydrogels have a relatively low level of complexity as
86 compared to most composite foods systems. They can be structurally manipulated in a
87 systematic manner, and exclude prior learning, emotional associations and expected
88 postprandial satisfaction (if any) during sensory testing.

89 Recently, there has been an increase in research efforts directed towards designing
90 hydrogels with structural complexity for various applications (Laguna & Sarkar, 2016;
91 Santagiuliana, et al., 2018; Tang, Larsen, Ferguson, & James, 2016). For instance, Laguna &
92 Sarkar (2016) demonstrated that incorporation of calcium alginate gel beads of 185-2380 μm
93 size in κ -carrageenan hydrogel matrix enabled to increase the oral residence time. On the other
94 hand, Tang, et al. (2016) showed the impact of using textural heterogeneity with seeds as well
95 as layering arrangements within gelatin-agar hydrogels on increasing satiation. Temporal
96 perception of texture contrast was recently investigated by Santagiuliana, et al. (2018), where
97 authors employed layering approaches to generate mechanical contrast in agar, κ -carrageenan,
98 and gelatine hydrogels and suggested that a combined effect of mechanical and

99 physicochemical properties influenced the dynamic perception of inhomogeneity over time.
100 Nevertheless, to our knowledge, creation of hydrogels with systematic manipulation of
101 structural complexity and understanding the impact of those manipulations on ‘chewing-’ and
102 ‘lubrication-’ related texture attributes that are perceived during early and later stages of oral
103 processing, respectively, have not been investigated to date.

104 The aim of this study was to understand the relationship between rheological,
105 tribological and sensory properties (n=11 panellists) of hydrogels differing in hydrocolloid
106 type, concentration and degree of inhomogeneity. Our hypothesis was that initial fracture
107 properties of the hydrogels and apparent viscosities of the gel boli could be correlated with
108 chewing-related texture attributes, whereas tribological properties (*i.e.* friction coefficients in
109 boundary and mixed lubrication) of the gel boli could be correlated with lubrication-related
110 texture attributes. A range of hydrogels using κ -carrageenan, locust bean gum (LBG), sodium
111 alginate and calcium alginate with different degrees of structural complexity and
112 inhomogeneity were employed to test this hypothesis.

113 κ -Carrageenan forms a tight-knit molecular network that results in the formation of a
114 strong homogenous gel matrix. Since real food is not homogeneous, a degree of structural
115 complexity was achieved in the samples by manipulating κ -carrageenan gels using LBG or
116 sodium alginate to form mixed gels. Incorporation of LBG can strengthen κ -carrageenan’s
117 continuous network, promoting elastic properties and reducing syneresis. This synergistic
118 interaction is attributed to the ability of LBG to form stable cross-links with κ -carrageenan
119 (Stading & Hermansson, 1993). On the other hand, sodium alginate is known to interfere with
120 the incipient coil-to-helix transition during the formation of the κ -carrageenan gel, and thus the
121 sodium alginate + κ -carrageenan mixture is expected to create a weaker mixed gel (Laguna &
122 Sarkar, 2016). To add another dimension to the structural complexity, a level of inhomogeneity
123 was introduced in the κ -carrageenan gels by inclusion of calcium alginate beads of different

124 particle sizes, where the latter behaved as “inactive filler particles” (Laguna & Sarkar, 2016).
125 Presence of calcium alginate beads would likely lead to a decrease of mechanical strength due
126 to interruption of the continuous κ -carrageenan network by these beads that acted as structural
127 defects. To our knowledge, this is the first study that attempts to examine the relationship
128 between rheology, tribology and sensory perception in hydrogels and findings from this study
129 should provide useful information for the design of novel foods with specifically tailored oral
130 texture and sensory properties.

131

132 **2. Materials and methods**

133 **2.1. Materials**

134 Food grade quality kappa-carrageenan, locust bean gum and sodium alginate were purchased
135 from Special Ingredients Ltd (Chesterfield, UK). Green food colouring was obtained from
136 AmeriColor (Placentia, USA) and American peppermint extract was purchased at a local
137 supermarket (Leeds, UK). Potassium chloride was purchased from Minerals Water Ltd
138 (Purfleet, UK) and calcium chloride from VWR International (Leuven, Belgium). Additionally,
139 sodium chloride, potassium phosphate, potassium citrate, uric acid sodium salt, urea, lactic acid
140 sodium salt, and porcine gastric Mucin Type II were obtained from Sigma-Aldrich (St. Louis,
141 USA). All materials were used without further purification. Demineralised water was used in
142 preparation for all the gels and the artificial saliva formulation.

143

144 **2.2. Preparation of the hydrogels**

145 The composition of the hydrogels is shown in **Table 1**. Visual images of the seven hydrogels
146 are shown in **Supplementary Figure 1**. Typically 400 g of sample was prepared and poured
147 into petri-dishes to a height of 2 cm (150 g gel per petri-dish), and then kept overnight at 4 °C.

148 Cylindrical pieces of the hydrogels were cut out from the petri-dish using a circular cookie
149 cutter (diameter 25 mm, height 10 mm), and used as such for all measurements.

150

151 *2.2.1. Kappa-carrageenan hydrogels*

152 For preparation of kappa-carrageenan hydrogels (κ C), appropriate quantities of κ C were
153 dispersed in a 0.2 M potassium chloride (KCl) solution and stirred for 30 min to ensure
154 maximum hydration. Then, the solution was heated up in a shaking water bath at 98 °C for 1
155 h. The gelling solutions were allowed to cool down for 5 min, and finally the green colouring
156 and peppermint flavouring were added before being allowed to set in petri-dishes.

157

158 *2.2.1. Kappa-carrageenan/ LBG or kappa-carrageenan/sodium alginate hydrogels*

159 The mixed hydrogels were prepared by mixing the appropriate quantities of powdered κ C and
160 LBG or sodium alginate (NaA) together before adding the respective powder mixtures to
161 distilled water and mixing for 30 min. Then, the solutions were heated up in a shaking water
162 bath at 98 °C for 1 h. The solutions were allowed to cool down for 5 min, and finally the green
163 colouring and peppermint flavouring were added before being allowed to set in petri-dishes.

164

165 *2.2.2. Kappa-carrageenan/calcium alginate hydrogels*

166 The calcium alginate (CaA) beads were prepared first and then added as a layer in the κ C
167 hydrogels (before the gels were allowed to set) to create a level of inhomogeneity within the
168 gels, based on a previous study (Laguna & Sarkar, 2016). The beads were prepared by making
169 a 1 wt% NaA solution in water, and stirring for 1 h to ensure complete hydration. Calcium
170 chloride (CaCl₂) solutions of 0.01 M and 0.05 M were prepared to make the 300 μ m and 1000
171 μ m sized beads, respectively. The 1 wt% NaA solution was passed through a Buchi
172 Encapsulator B-390[®] (Buchi UK Ltd, Chadderton, UK) with a vibrating nozzle and then

173 dropped into the appropriate CaCl_2 solutions while being stirred to create the CaA beads. A
174 vibrating nozzle of $300\ \mu\text{m}$ (frequency 500 Hz, air pressure 250 mbar) or $1000\ \mu\text{m}$ (frequency
175 700 Hz, air pressure 300 mbar) was used depending on the required bead size. The beads were
176 allowed to set in the CaCl_2 solution at room temperature for 30 min under constant stirring.
177 The beads were subsequently washed thrice with distilled water and then air-dried. Meanwhile,
178 the κC solution was prepared by dissolving the appropriate amount in distilled water and
179 mixing for 30 min. Then, the solution was heated up in a shaking water bath at $98\ ^\circ\text{C}$ for 1 h
180 and allowed to cool down for 5 min followed by adding the green colouring and peppermint
181 flavouring. The appropriate amount of CaA beads was weighed and added to the petri-dish and
182 the κC gels solution was poured, before allowing the gel to set similar to the preparation method
183 of the aforementioned hydrogels.

184

185 **2.3. Texture analysis**

186 Uniaxial single compression tests were carried out using a TA-TX2 Texture Analyzer (Stable
187 Micro Systems Ltd., Surrey, UK), attached with a 50 kg load cell. In the compression test, the
188 samples were compressed using a cylindrical probe (diameter 59 mm). The tests were carried
189 out at $22\ ^\circ\text{C}$, at a constant speed of 2 mm/sec and the deformation level was set at 80 % strain.
190 At least three repeats were recorded for each gel on at least four different gel preparation days.
191 The software Exponent (TEE32, v6.1.9.0, Stable Micro Systems Ltd., Surrey, UK) was used
192 to obtain the force-distance curves, and the fracture mechanics were calculated from these
193 curves. The fracture properties were determined at the maximum point of the stress-strain
194 curves. The fracture energy was determined as the area under the curve up to the fracture point
195 (Peleg, 1984). The initial slope of all samples was determined up to a stress of 500 Pa, as this
196 was considered within the viscoelastic limit.

197

198 **2.4. Preparation of artificial saliva**

199 Artificial saliva was prepared according to the method previously described by Sarkar, et al.
200 (2009). Briefly, artificial saliva was composed of 0.16 g/L NaCl, 0.33 g/L NH₄NO₃, 0.64 g/L
201 K₂HPO₄, 0.2 g/ L KCl, 0.31 g/L K₃C₆H₅O₇.H₂O, 0.02 g/L C₅H₃N₄O₃Na, 0.2 g/L H₂NCONH₂,
202 0.15 g/ L C₃H₅O₃Na and 3 g/L mucin. The pH of the saliva solution was adjusted to pH 6.8
203 using 1 M NaOH. Noteworthy, porcine mucin was used in the artificial saliva to simulate the
204 human salivary viscosity at comparable concentrations present in human saliva. However,
205 bovine submaxillary mucin could be a promising alternative considering its ability to form
206 more elastic films and its higher lubricating properties particularly in elastomeric contact
207 surfaces (Madsen, et al., 2016).

208

209 **2.5. Simulated oral processing**

210 The hydrogels were broken down mechanically in the presence of artificial saliva to mimic oral
211 processing. The samples were put into a mechanical blender (Andrew James UK Ltd, Bowburn,
212 UK) with artificial saliva in a ratio 2:1 w/w and homogenized for 15 seconds at low speed
213 (speed 1). Depending on the hydrogel tested, the obtained particle size was < 2-5 mm. After
214 grinding, the gel was mixed with artificial saliva (final sample to saliva ratio 4:3 w/w) and left
215 to rest for 30 min. It is worth highlighting that the amount of saliva incorporated in the food
216 bolus has varied across studies from as low as 8 wt% saliva *in vivo* in emulsion gels (Devezeaux
217 de Lavergne, van de Velde, van Boekel, & Stieger, 2015a) to 18 wt% artificial saliva
218 incorporation *in vitro* to create model hydrogel boli (Ishihara, Nakauma, Funami, Otake, &
219 Nishinari, 2011) to 50 wt% simulated saliva addition for food matrices in case of harmonized
220 INFOGEST static model (Minekus, et al., 2014). For our study, we used a ratio of 4:3 (w/w)
221 sample:saliva to have the same level of saliva incorporation across all samples to enable
222 comparison, though we highlight the limitation that during oral processing (*in vivo*), the amount

223 of saliva added to the samples would not be the same across the different hydrogels with
224 varying degrees of complexity.

225 The broken down hydrogel:saliva mixture samples, from here on defined as ‘gel bolus
226 fragments’, were used for the rheological and tribological measurements. To understand the
227 thin-film properties, the tribological properties were also measured for the samples where any
228 large gel particles (> 500 μm) were filtered out, from here on defined as ‘gel bolus filtrate’.

229

230 **2.6. Apparent viscosity**

231 The apparent viscosities of the gel fragments in presence of artificial saliva were
232 measured using a rheometer (Kinexus Ultra+, Malvern Instruments Ltd, Worcestershire, UK)
233 equipped with a plate-plate geometry (diameter 60 mm). The gap size (ranging from 0.01-0.15
234 mm) was individually adjusted for each gel, depending on their particle size once broken down.
235 To prevent evaporation, the samples were sealed off with a thin layer of silicone oil. Flow
236 curves were obtained for all gel samples after simulated oral processing at shear rates ranging
237 from 0.0001 to 100 s⁻¹ at 37 °C. A minimum of three measurements were performed for each
238 sample. Associated Ostwald de Waele power law (equation (1)) was fitted to the viscosity of
239 each sample:

240

$$241 \quad \eta = K\dot{\gamma}^{n-1} \quad (1)$$

242

243 where η is the apparent viscosity, K is the consistency index (Pa s) and n is the behaviour index.
244 These parameters were utilised in the determination and validation of the corresponding
245 viscosities calculated by entrainment speeds and permitted friction coefficients to be plotted
246 against the entrainment speed and viscosity products as described in the tribology section.

247 It is noteworthy that detailed rheological characterization of the viscoelasticity of the hydrogels
248 and the corresponding bolus fragments was not carried out in this study.

249

250 **2.7. Oral tribology**

251 The oral tribological properties of the gel bolus fragments and gel bolus filtrates were
252 determined using a ball-on-disc set up in a Mini Traction Machine (MTM2, PCS Instruments,
253 London, UK). The gel bolus samples were prepared according to the method described above.
254 Commercially available polydimethylsiloxane (PDMS) ball (diameter of 19 mm, MTM ball
255 Slygard 184, 50 Duro, PCS Instruments, London, UK) and disc (diameter of 46 mm, thickness
256 of 4 mm, MTM disc Slygard 184, 50 Duro, PCS Instruments, London, UK) were used for the
257 measurements (surface roughness of PDMS tribopairs, $R_a < 50$ nm). The PDMS surface
258 contacts were kept a minimum of 2 h submerged in artificial saliva to create a mucin film with
259 the intent to simulate the oral conditions. The sample was loaded into the pot equipped with
260 the PDMS disc; the ball was lowered onto the disc and then the pot was covered with a lid. The
261 PDMS ball and disc were rotated at different speeds to create a relative motion between the
262 surface of the ball and the disc, resulting in a slide-to-roll ratio (SRR) of 50%, to impart both
263 rolling and sliding motions (Sarkar, et al., 2017a) and the temperature was maintained at 37
264 °C, simulating oral conditions.

265 Two parameters have been used for both the ball speed and the disc speed: one with
266 $V_{ball} > V_{disc}$ and one with $V_{ball} < V_{disc}$, while keeping the SRR constant. The entrainment speed
267 was calculated as the average of the two measures to remove any offset errors in the lateral
268 force measurement, as well to remove any friction that did not reverse sign when the speeds
269 were reversed, such as rolling friction (Bongaerts, Fourtouni, & Stokes, 2007a). Thus, the
270 entrainment speed was defined as:

271

272
$$\bar{U} = \frac{1}{2}(U_1 + U_2) \quad (2)$$

273

274 where U is the entrainment speed and U_1 and U_2 are the velocities of the two contacting
 275 surfaces (i.e. ball and disc). The rolling speed was reduced from 1000 to 1 mm/s and friction
 276 forces were measured to obtain a Stribeck curve. All tests were performed at a load of 2 N, as
 277 this is a good representative value of loads occurring in the mouth while maintaining sensitivity
 278 in the tribometer. Average and standard deviation were calculated from three measurements on
 279 replicate samples. Following the studies by de Vicente, StokesSpikes (2005) and Bongaerts, et
 280 al. (2007a), we utilized the Stribeck ‘master curve’ (equation 3) to enable comparison of sample
 281 friction coefficient μ against the product of entrainment velocity U and sample viscosity η :

282

283
$$\mu_{total} = \mu_{EHL} + \left(\frac{\mu_b - \mu_{EHL}}{1 + (U\eta/B)^m} \right) \quad (3)$$

284

285 where

286

287
$$\mu_{EHL} = k(U\eta)^n \quad (4)$$

288

289 and

290

291
$$\mu_b = h(U\eta)^l \quad (5)$$

292

293 where, (k, n) and (h, l) are the elastohydrodynamic lubrication (EHL) and boundary layer power
 294 law coefficient and index respectively. Here, B relates to the threshold value of $U\eta$ for boundary
 295 friction and m represents the mixed regime exponent. It is worth pointing out that the flow

296 curves (in the above section) were only determined for gel fragments to relate to the early stages
297 of oral processing where bulk properties tend to dominate. However, friction coefficients were
298 determined for both bolus fragments and filtrates, latter resemble the thin layer formed between
299 the contact surfaces (*e.g.* tongue and palate) in later stages of oral processing, where surface
300 properties dominate (Chen & Stokes, 2012; Laguna & Sarkar, 2017; Stokes, et al., 2013).

301

302 **2.8. Descriptive sensory analysis**

303 A panel was recruited from the University of Leeds to participate in a descriptive sensory
304 analysis. The panel was selected and familiarized with the hydrogel samples followed by
305 generation of attributes and introduction to the used rating scale. The study was reviewed and
306 approved by the Faculty Research Ethics Committee at the University of Leeds (ethics
307 reference MEEC 16-006). A group of 11 participants (4 male, mean (\pm SD) age = 28.8 (\pm 5.5)
308 years, range 21-40 years) was trained to familiarize them with the different hydrogel samples
309 and to create a list of relevant attributes related to the chewing as well as the lubrication aspects
310 of the gels.

311 Three training sessions of 1 h each were conducted with the seven hydrogel samples.
312 During the first training session, the hydrogels were tasted to familiarise the participants with
313 the type of samples, and participants were encouraged to come up with terms to describe the
314 different texture aspects of the different gels. Subsequently, an extensive list of potential
315 attributes related to both the chewing and lubrication aspects was introduced to the participants
316 and their applicability and definitions were discussed in the group. During the second session,
317 the list of attributes generated during the first training session was further specified to describe
318 the difference between the textural aspects of the gels as best as possible and to reach a
319 consensus within the panel. Finally, in the last training session the rating scales were introduced

320 and a group discussion resolved how to use the scales for the different attributes in the included
321 samples and the best order in which to rate these attributes.

322 After completion of the training, the samples were evaluated in individual sensory test
323 booths under normal lighting conditions, with the samples presented in randomised order in
324 triplicate in a balanced block design divided over two test days (with 11 samples rated on day
325 one and 10 samples on day two). All samples were prepared 24 h prior to the sensory
326 assessment, presented in individual cups labelled with a three-digit code, and moved to room
327 temperature 20 min before the start of the test. A practice sample was provided on each test
328 day to get a sense of the samples before the start of the test due to the novelty of these hydrogels.
329 As determined by the training sessions, nine different texture attributes were rated for each
330 sample in a fixed order (see **Table 2**).

331 The intensities of the different attributes were rated onto an unstructured line scale of 100
332 mm, as presented with the software CompuSense (v5.0, Ontario, Canada), anchored from ‘not
333 at all’ (0) to ‘very’ (100). All panellists followed the same tasting procedure, putting the sample
334 as a whole in the mouth. It was optional for the panellists to choose whether to swallow the
335 sample at the end or spit it out in provided cups. Between each sample, panellists were
336 instructed to rinse their mouth with water and eat a cracker to cleanse their palate. Data was
337 extracted from the software and exported to SPSS (IBM® SPSS® Statistics, v24, SPSS Inc,
338 Chicago, USA) for analysis.

339

340 **2.9. Statistical analysis**

341 Mean values and standard deviations (SD) were calculated using Excel (Microsoft Office
342 2010). For each sample, sensory attribute and assessor in the sensory analysis, the panel
343 performance was checked to make sure there were no clear outliers or obvious errors using the
344 software PanelCheck (v1.4.2). The panel performance was assessed and panel agreement,

345 discrimination and repeatability among assessors was considered to be acceptable according to
346 the Tucker-1, F- and MSE-plots, respectively (Tomic, et al., 2010), and thus, no data was
347 removed.

348 In addition, Principal Component Analysis (PCA) was conducted on the nine sensory
349 attributes with orthogonal rotation (Direct Oblimin). The Kaiser-Meyer-Olkin measure verified
350 the sampling adequacy for the analysis: $KMO = 0.788$, which is well above the acceptable limit
351 of 0.5 (Field, 2017). Bartlett's test of sphericity $\chi^2 (36) = 1197.985$, $p < .001$, indicated that
352 correlations between items were sufficiently large for PCA. An initial analysis was run to
353 obtain eigenvalues for each component in the data. Two components had Eigenvalues over
354 Kaiser's criterion of 1 and in combination explained 64.1% of the variance, and thus were
355 retained in the final analysis.

356 In order to study the differences in samples for all selected attributes, analysis of variance (one-
357 way ANOVA) was applied to the ratings data from the sensory panel with the samples as fixed
358 factor; least significant differences were calculated by Bonferroni's post-hoc test. Similarly,
359 differences between samples for the mechanical analyses (uniaxial compression test of
360 hydrogels, flow curves of bolus fragments, friction coefficients of gel bolus fragments and
361 filtrates) were determined with one-way ANOVA and Bonferroni post-hoc testing. Pearson's
362 product moment correlations were calculated to assess the simple relationships between the
363 different instrumental and sensory characteristics of the hydrogels. All statistical analyses were
364 performed in SPSS (IBM® SPSS® Statistics, v24, SPSS Inc, Chicago, USA), and statistical
365 significance level was set at $p < 0.05$.

366 3. Results and discussion

367 3.1. Mechanical characterisation of hydrogels and simulated boli

368 3.1.1. Texture analysis of the hydrogels

369 The fracture stress and strain of the seven hydrogels are shown in **Figure 1**. The samples
370 can be categorized into three groups: 1) high fracture stress/high fracture strain, 2) intermediate
371 fracture stress/fracture strain, and 3) low fracture stress/low fracture strain. Group 1 included
372 the two κ C samples (2 wt% and 3 wt%) and the κ C/LBG sample, averaging a fracture stress of
373 190 kPa and a fracture strain of 1.17. Group 2 included the samples containing the CaA beads,
374 with an average fracture stress and fracture strain of 71 kPa and 0.93, respectively, where the
375 particle size of CaA beads (300 or 1000 μ m) did not show any significant contribution to the
376 fracture mechanics at equivalent biopolymer concentration ($p > 0.05$). Group 3 consisted of
377 the κ C/NaA hydrogels with an average fracture stress of 27 kPa and a fracture strain of 0.70.
378 The high and low fracture stress samples varied by a factor 7 and the samples in the low and
379 high fracture strain groups varied by a factor 1.8. The fracture energy of the hydrogels, shown
380 in **Supplementary Table 1**, also indicate that the samples were categorized in similar groups
381 as in **Figure 1**. Based on these groupings, **Figure 2** shows a schematic representation of the
382 structures of these hydrogels.

383 As expected, the fracture stress followed a power law increase with increased
384 concentration of κ C in native κ C hydrogels (**Figure 1**), allowing the formation of a three-
385 dimensional network structure (as shown schematically in **Figure 2**) induced by the
386 supramolecular aggregation of the double helices (Laguna & Sarkar, 2016). Interestingly, the
387 fracture stress of the 2.25 κ C0.75LBG hydrogel was significantly lower than that of 3 κ C
388 hydrogel at equivalent total biopolymer concentration ($p < 0.05$). This is not in line with
389 previous findings, where it has been reported that LBG has the ability to strengthen the κ C
390 network by forming multiple junction zones between LBG un-substituted mannan backbones

391 and κ C helices (Dea & Morrison, 1975; Devezeaux de Lavergne, Strijbosch, Van den Broek,
392 Van de Velde, & Stieger, 2016; Dunstan, et al., 2001). A possible explanation for this could be
393 the difference in total biopolymer concentrations and the ratio between κ C and LBG used in
394 this study versus previous reports. Interestingly, Czaczyk, OlejnikTrojanowska (1999) also
395 observed similar weakening effect of LBG on κ C hydrogels at 2-3 wt% total biopolymer
396 concentration in a ratio of κ C: LBG of 2:1 w/w *i.e.* similar to the range used in this study.

397 Unsurprisingly, the presence of NaA (1.5 κ C0.5NaA hydrogel) resulted in significant
398 weakening of the κ C gel (**Figure 1**), which might be attributed to the segregative interaction
399 between NaA and κ C, disrupting the coil-to-helix transition during κ C hydrogel formation
400 (**Figure 2**), finally leading to a phase separated κ C/NaA hydrogel (Goh, Sarkar, & Singh, 2008,
401 2014; Laguna & Sarkar, 2016). On the other hand, the presence of CaA beads (1.6 κ C0.2CaA₃₀₀,
402 1.6 κ C0.2CaA₁₀₀₀) contributed to considerable reinforcement of the κ C hydrogel as compared
403 to that of the presence of NaA (1.5 κ C0.5NaA). Introducing defects due to the presence of these
404 CaA beads as “inactive filler particles”, resulted in a less defined network (**Figure 2**) with less
405 fracture stress as compared to that of a native κ C hydrogel (**Figure 1**). Based on the texture
406 analysis results, it can be concluded that the chosen hydrogel types covered a wide range of
407 deformation behaviour, which can be hypothesized to have different sensory properties,
408 particularly in terms of chewing-related attributes.

409

410 3.1.2. Apparent viscosity of the hydrogel bolus

411 **Figure 3** shows the apparent viscosity (η) of the bolus particles derived from simulated oral
412 processing of the hydrogels in the presence of artificial saliva at 37 °C. All bolus fragments in
413 presence of artificial saliva showed extreme shear thinning behaviour, with slight indications
414 of plateau values being reached only at low shear rate limits (10^{-3} s^{-1}). Such pseudoplastic

415 behaviour is in agreement with that of protein-based microgels, where latter showed similar
416 ranges of η values as a function of volume fraction and shear rate (Sarkar, et al., 2017a).

417 In addition, high values of η persisted in boli of both κ C hydrogels and mixed hydrogels
418 even after subjection to fairly high *i.e.* orally relevant shear of 50 s^{-1} . As expected, due to the
419 aforementioned segregative interaction between κ C and NaA, the bolus of $1.5\kappa\text{C}0.5\text{NaA}$
420 hydrogels were one to two orders of magnitude lower in η as compared to that of the rest of the
421 hydrogels (κ C, κ C/LBG and κ C/CaA) even though all the systems were highly shear thinning.
422 It is worth noting that at oral shear (50 s^{-1}), η of $1.5\kappa\text{C}0.5\text{NaA}$ hydrogel bolus fragments and
423 the rest of the (κ C, κ C/LBG and κ C/CaA) hydrogel bolus fragments was three or four orders
424 of magnitude higher than artificial saliva (**Figure 3**) or real human saliva, respectively
425 (Bongaerts, Rossetti, & Stokes, 2007b). This suggest that the rheology might play an important
426 role in driving the load bearing capacity of these gel bolus fragments during oral tribology
427 experiments and consequently sensory perception. However, viscosity results might not be
428 sufficient to understand the underlying mechanism of differences in the friction coefficients (if
429 any) between κ C, κ C/LBG and κ C/CaA hydrogel bolus, as the viscosities were not significantly
430 different between these gel bolus fragments at orally relevant shear rates ($p > 0.05$).
431 Furthermore, one might investigate how the viscoelastic parameters of the bolus fragments may
432 impact the load bearing aspects and oral processing attributes, which is beyond the scope of
433 this study and needs to be studied in future.

434

435 3.1.3. Oral tribology of the hydrogel bolus fragments and filtrates

436 It is well recognized that the rheological properties (bulk phase) dominate the textural sensation
437 only in the early stages of oral processing. It is now postulated that oral tribology (surface
438 properties) dictates the thin-film properties and thus the oral sensation in the later stages of oral
439 processing where the food and/or food-saliva mixture interact with the oral surfaces (Chen &

440 Stokes, 2012; Laguna & Sarkar, 2017; Pradal & Stokes, 2016; Stokes, et al., 2013). To
441 understand this surface phenomenon, the coefficient of friction (μ) of both gel bolus fragments
442 and gel bolus filtrate (*i.e.* the thin-film) when sheared between smooth hydrophobic PDMS-
443 PDMS ball and disc tribopairs was plotted as a function of entrainment speed as shown in
444 **Figures 4a** and **4b**, respectively. Although attempts were made to pre-adsorb artificial salivary
445 films to hydrophobic PDMS substrates, there was no change in the water contact angle (θ) of
446 the substrates (data not shown) and the PDMS surface remained hydrophobic ($\theta = 108^\circ$) as
447 studied previously (Sarkar, et al., 2017a; Yakubov, McColl, Bongaerts, & Ramsden, 2009).

448 The plateau boundary ($\bar{U} \leq 10$ mm/s) and mixed regimes ($10 < \bar{U} \leq 300$ mm/s) of
449 lubrication could be clearly identified in the Stribeck curves of the measured samples (**Figures**
450 **4a** and **4b**). Considering the relevance of biologically relevant speeds, such as the speed of the
451 human tongue being ~ 20 mm/s (Steele & Van Lieshout, 2009), we have focussed only on
452 boundary and mixed lubrication regimes. The artificial saliva, which served as a control,
453 showed a classical Stribeck profile with μ varying from 0.3–0.5 in the boundary regime, falling
454 off by one-order of magnitude in the mixed regime. This is consistent with ranges of values
455 found in a previous study using the same artificial saliva formulation (Laguna, et al., 2017a).

456 In the boundary conditions, the PDMS ball and disc appeared to be in near-adhesive
457 PDMS-PDMS (intimate) contact, where the entrainment of the hydrogel bolus fragments or
458 filtrates was rather poor (**Figures 4a** and **4b**). Interestingly, gel fragments containing higher
459 concentration of κC ($3\kappa\text{C}$), LBG ($2.25\kappa\text{C}0.75\text{LBG}$) and alginates as beads ($1.6\kappa\text{C}0.2\text{CaA}_{1000}$,
460 $1.6\kappa\text{C}0.2\text{CaA}_{300}$, $2.4\kappa\text{C}0.2\text{CaA}_{300}$) showed some sort of entrainment even in the boundary
461 regime reducing the friction force significantly (< 0.4 N) as compared to that of artificial saliva
462 ($p < 0.05$) (**Table 3**). Gong & Osada (1998) described a “repulsion–adsorption model” to
463 explain friction in hydrogels, which suggests that the friction force is the sum of elastic force
464 and viscous force, which can be applied to these gel bolus fragments. The elastic force arises

465 from anchorage of the biopolymer to the substrate (adhesive), whereas the viscous force results
466 from the hydration of the polymer (repulsive) (Gong & Osada, 1998; Gong, 2006; Stokes,
467 Macakova, Chojnicka-Paszun, de Kruif, & de Jongh, 2011). At a first glance, it seems that the
468 reduction in μ in the boundary regime of these gel fragments (3 κ C, 2.25 κ C0.75LBG,
469 1.6 κ C0.2CaA₁₀₀₀, 1.6 κ C0.2CaA₃₀₀, 2.4 κ C0.2CaA₃₀₀) might be associated with interactions
470 between κ C, LBG, NaA or CaA hydrogels and the PDMS substrates allowing biopolymer
471 adsorption to some degree. However, this is somewhat unlikely considering the high
472 hydrophobicity of PDMS (Sarkar, et al., 2017a) and hydrophilicity of these gels.

473 Hence, the relevance of ‘opposing substrate’ in friction in this case is worth recognizing
474 (Gong, Kagata, Iwasaki, & Osada, 2001). Note, both κ -carrageenan and alginates are highly
475 negatively-charged biopolymers at pH 6.8. Thus, repulsions from both opposing PDMS
476 substrates (artificial saliva coated *i.e.* negatively charged) (Sarkar, et al., 2009; Sarkar, et al.,
477 2017a) as well as the opposing gel surfaces (*i.e.* inter-gel repulsion between negatively-charged
478 gel bolus fragments) (Bongaerts, Cooper-White, & Stokes, 2009; Gong, Kagata, & Osada,
479 1999; Gong & Osada, 2002) are highly likely. Such repulsive interactions against the opposing
480 artificial saliva coated PDMS substrate and/or the gel fragment surfaces, might have enabled
481 these hydrogel fragments to remain hydrated forming a thicker solvent layer of ‘lubricant’, thus
482 providing an effective barrier to the asperity contacts under the low load. This is further
483 justified by the high viscosity values of these specific gel fragments (**Figure 3**) suggesting
484 viscous force as the driving factor and separating the PDMS contacts effectively (**Figure 4a**).

485 As the sliding speed of the disc started to increase, μ decreased in all samples (**Figures**
486 **4a and Figures 4b**) and started to fill the gap between the surface asperities of the tribopairs
487 in the mixed lubrication regime. The inclusion or exclusion of gel fragments or gel filtrate
488 largely depends on the gap between the contacting surfaces, the size of the gel fragments
489 compared to the size of the gap and asperities, as well as the interactions of these gel fragments

490 with the PDMS surfaces. In the case of gel bolus fragments containing beads (1.6κC0.2CaA₁₀₀₀,
 491 1.6κC0.2CaA₃₀₀, 2.4κC0.2CaA₃₀₀) (**Figure 4a**), the μ was one-order of magnitude lower than
 492 artificial saliva ($p < 0.05$). The beads were larger in size as compared to the asperities of the
 493 PDMS substrates ($R_a = 50$ nm) and thus the beads released from the gel fragments during
 494 simulated oral processing might have rolled into the contact zone between the PDMS
 495 tribopairs, thus reducing μ values. It is tempting to propose a “ball-bearing mechanism” for the
 496 reduction in μ using CaA, such mechanism has been previously postulated for whey protein
 497 particles and protein microgel particles (Liu, Tian, Stieger, van der Linden, & van de Velde,
 498 2016; Sarkar, et al., 2017a).

499 To test the possibility of this ball-bearing mechanism occurrence, the Hertz pressure
 500 effects for the CaA beads of 1000 and 300 μ m were calculated with the assumption that 10%
 501 of the beads were entrained between the PDMS ball and disc surfaces (de Vicente, et al., 2005;
 502 Johnson, 2009; Johnston, McCluskey, Tan, & Tracey, 2014; Puttock & Thwaite, 1969). The
 503 Young’s modulus for CaA beads was assumed to be 20 kPa, based on previous studies (Larsen,
 504 Bjørnstad, Pettersen, Tønnesen, & Melvik, 2015). From Hertz theory, the spherical contact area
 505 of the PDMS ball and disc was calculated using Eq (3):

$$506 \quad \pi\alpha^2 = 1.31 \left(\frac{R'F}{E'} \right)^{0.67} \quad (3)$$

507
 508 where, α is the surface contact, R' is the reduced radius of the PDMS ball, F is the force for
 509 each particle entrained between the two contacts and E' is the reduced elastic modulus. The E'
 510 was defined as:

$$511 \quad \frac{2}{E'} = \frac{1-\sigma_1^2}{E_1} + \frac{1-\sigma_2^2}{E_2} \quad (4)$$

513

514 where, σ is the Poisson's ratio, assumed to be 0.5, and E is the Young's modulus (de Vicente,
515 et al., 2005).

516 The number of particles in the contact area was calculated as:

517

$$518 \quad N_{particles} = \frac{\varphi_{particles} \times A}{\pi R^2} \quad (5)$$

519 with φ being the concentration of particles in the contact zone, A the area of contact ($\pi\alpha^2$) and
520 R the radius of the particles. Hence, the force per particle was calculated as:

521

$$522 \quad F_{particle} = \frac{F_{total}}{N_{particles}} \quad (6)$$

523

524 with F the total force applied and N the number of particles. Finally, the spherical contact area
525 was determined using the approach of distant points (Johnson, 2009):

526

$$527 \quad \alpha = \left(\frac{9F^2}{16R'E'^2} \right)^{1/3} \quad (7)$$

528

529 with E' defined as:

$$530 \quad E' = 2 \left(\frac{1-\sigma_1^2}{E_1} + \frac{1-\sigma_2^2}{E_2} \right)^{-1} \quad (8)$$

531

532 The results shown in **Table 4** clearly indicate that the CaA particles were not capable
533 of rolling as $\alpha \gg$ size of the beads, even with 10% particles being entrained between the PDMS
534 surfaces. Interestingly, the 1000 μm CaA beads were too large to actually be entrained in the
535 contact zone. These calculations indicate that there was no “ball-bearing effects” using CaA

536 irrespective of the particle size studied, and the reduction in μ could be explained by the
537 rheological behaviour (**Figure 3**) of the gel boli containing beads forming the viscous layer as
538 the ‘lubricant’, as discussed previously. Also, not to underestimate, that the amount of water
539 within these gel beads might also play an important role in exhibiting low friction (Gong &
540 Osada, 2002). The water might be squeezed out the gel beads forming a thin-film and may
541 serve as a ‘boundary lubricant’.

542 In case of the gel filtrates (**Figure 4b**), the Stribeck curve of the κ C hydrogels almost
543 overlapped irrespective of the biopolymer concentration in both boundary and mixed
544 lubrication regimes ($p > 0.05$). Similarity in friction forces for both 2κ C and 3κ C hydrogel
545 bolus filtrates and artificial saliva irrespective of entrainment speeds (**Table 3**) suggests that
546 the hydrogel bolus filtrates lacked the ability to migrate into and replenish the confined region
547 in the event that the two PDMS shearing surfaces were almost in direct contact. This is unlike
548 the behaviour in **Figure 4a**, where κ C gel bolus fragments showed entrainment driven by the
549 viscosity of the hydration layer created by the gel bolus fragments (**Figure 3**). As expected,
550 such influence of rheology on tribology was not evident in the hydrogel bolus filtrates owing
551 to the loss of the gel fragments particles during filtration (**Figure 4b**). In the mixed lubrication
552 regime, the filtrates from hydrogel boli containing LBG (2.25κ C 0.75 LBG), NaA
553 (1.5κ C 0.5 NaA) or CaA (1.6κ C 0.2 CaA $_{1000}$, 1.6κ C 0.2 CaA $_{300}$, 2.4κ C 0.2 CaA $_{300}$) contributed to
554 significantly lower friction forces as compared to the artificial saliva ($p < 0.05$) (**Table 3**). This
555 complies with the behaviour observed for the corresponding hydrogel bolus fragments (**Figure**
556 **4a**). Even after filtration, the spherical CaA beads might have been retained in the filtrate
557 enabling some degree of entrainment (**Table 4**), or both gel fragments containing NaA and
558 CaA were increasing the lubrication effect, possibly by ‘weeping out’ the water layer as a thin-
559 film ‘boundary lubricant’ (Gong & Osada, 2002).

560 In our study, the fitted values with the Stribeck master curve *i.e.* $k = 0.0065$, $n = 0.55$,
561 $h = 11$, $l = 0.075$, $B = 0.33 \cdot 10^{-4}$, $m = 1.0$ gave a good fit (Bongaerts, et al., 2007a; de Vicente,
562 et al., 2005). Here it should be noted that since the samples were shear thinning (**Figure 3**), the
563 viscosity multipliers were calculated at each entrainment velocity. This was achieved by fitting
564 the entrainment speeds to the shear rate by use of a power law relation of the same format as
565 Eq (7), and which enabled calculation of the associated viscosity. In this study, entrainment
566 speeds of 1 to 1000 mm/s translated to shear rates of 0.1 - 100 s⁻¹. This was validated to ensure
567 the entrainment speeds did indeed coincide with shear rates and that the predicted viscosities
568 agreed with the shear rate/viscosity Ostwald de Waele power law regressions relevant to each
569 sample.

570 As can be seen in the master curve (**Figure 5**), good agreement was achieved in the
571 mixed regime and from the transitional region into the EHL. However, in contrast to
572 Newtonian lubricants (Bongaerts, et al., 2007a; de Vicente, et al., 2005), using the particulate
573 hydrogel bolus fragments, the model failed in the boundary regime. This suggests that the
574 hydrogel bolus particles had a different degree of entrainment in the boundary regime and the
575 key mechanism of friction reduction in the boundary regime was due to opposing surface-
576 mediated formation of a viscous layer of ‘gel fragments’ (**Figure 4b**). As one might expect,
577 such layer formation varied as a function of sample inhomogeneity under shear conditions in
578 confinement and samples with inhomogeneity indicated a limitation in the Stribeck
579 representation in this regime.

580

581 **3.2. Descriptive sensory analysis of the hydrogels**

582 **Table 2** summarizes the sensory attributes generated by the sensory panel together with their
583 definitions. Nine different texture attributes were selected that were perceived during oral
584 processing of the hydrogels. With the first two principal components (PC), 64% of the variance

585 in the data was explained and the PCA plot showed that attributes were clustered in three groups
586 (**Figure 6**). The pattern matrix, **Table 5**, shows that PC1 included the attributes related to the
587 chewing aspects: ‘firm’, ‘elastic’, ‘chewy’ and ‘cohesive’, as well as the inverse of the
588 attributes more related to lubrication: ‘pasty’ and ‘melting’. The PC2 was represented by
589 attributes that could be considered in the oral lubrication domain: ‘smooth’, ‘slippery’ and
590 ‘salivating’. At first bite, perceived firmness of a solid or semi-solid food is known to be related
591 often to the fracture stress (Foegeding, et al., 2011). In fact, in this study, for all the chewing-
592 related attributes (see **Figure 7**), the hydrogels could be categorised into two key groups. Group
593 1) included the hydrogels with high fracture stress/high fracture strain (κ C and κ C/LBG gels)
594 (**Figure 1**) that generally scored high on the chewing-related texture attributes, such as ‘firm’,
595 ‘elastic’ and ‘cohesive’, and Group 2) included the hydrogels with low fracture stress/low
596 fracture strain (κ C/NaA and κ C/CaA gels) that scored low on these attributes. As one might
597 expect, the chewing-related texture attributes were strongly dominated by the concentration of
598 κ C *i.e.* higher concentration of κ C (3wt%) resulted in more ‘firm’ and ‘chewy’ perception as
599 compared to that created using lower concentrations (2 wt%) ($p < 0.05$). Similarly for samples
600 containing beads of the same size (300 μ m), a higher concentration of κ C (2.4 wt%) resulted
601 in creating samples (2.4 κ C0.2CaA₃₀₀) that scored on the higher end of the 100 mm scale and
602 were more ‘firm’, chewy’, ‘elastic’ and ‘cohesive’, as compared to that created using lower κ C
603 concentrations (1.6 wt%) ($p < 0.05$). Although the presence of beads and their particle size
604 (300 versus 1000 μ m) significantly influenced the fracture mechanics during the uniaxial
605 compression test (**Figure 1**), this was not apparent in the sensory analysis of the four chewing-
606 related texture attributes ($p > 0.05$) (**Figure 7**).

607 The lubrication-related texture attributes (see **Figure 8**) appeared to show a somewhat
608 opposite effect, with the low fracture stress/low fracture strain samples scoring high on
609 ‘melting’ and ‘pasty’, whereas the high fracture stress/high fracture strain samples scored

610 relatively low on the 100 mm scale. The $\kappa\text{C}/\text{NaA}$ hydrogel (1.5 κC 0.5NaA) scored high on most
611 of the lubrication-related texture attributes, such as ‘smooth’, ‘pasty’, ‘melting’. It is worth
612 remembering that the 1.5 κC 0.5NaA hydrogel bolus had the lowest η (though three-orders of
613 magnitude higher than human saliva) as compared to the other samples (**Figure 3**).
614 Nevertheless, the higher scores on the lubrication-related texture attributes of the $\kappa\text{C}/\text{NaA}$
615 hydrogel is in close agreement with the lower μ values (**Figure 4b**), and correspondingly lower
616 friction force in both boundary and mixed lubrication regimes for the hydrogel bolus filtrate
617 (**Table 3**). This suggests that the viscosity-parameter could not explain the lubrication-related
618 texture attributes in case of $\kappa\text{C}/\text{NaA}$ hydrogel and it was the ‘weeping’ water film that might
619 have acted as a ‘boundary lubricant’. Interestingly, the κC and $\kappa\text{C}/\text{LBG}$ hydrogels scored
620 significantly low on ‘pasty’ and ‘melting’ ($p < 0.05$), congruent with the high μ of the hydrogel
621 bolus filtrate (**Figure 4b**) and their correspondingly high friction forces in both the boundary
622 and mixed regimes (**Table 3**).

623 The $\kappa\text{C}/\text{CaA}$ hydrogels with beads (1.6 κC 0.2CaA₃₀₀, 1.6 κC 0.2CaA₁₀₀₀,
624 2.4 κC 0.2CaA₃₀₀) scored rather intermediate (30-60 mm) on all lubrication attributes. They
625 were perceived to be more ‘melting’ and ‘pasty’ as compared to the κC and $\kappa\text{C}/\text{LBG}$ hydrogels
626 ($p < 0.05$) (**Figure 8**), which corresponds with the reduced friction coefficients (**Figure 4b**)
627 and equivalent friction force in the mixed regime for these samples (**Table 3**). However,
628 considering that these beads were not rolling, as discussed before, the beads appeared to
629 provide some degree of inhomogeneity perception, which might explain the relatively low
630 scores on the attribute ‘smooth’ ($p < 0.05$) as compared to that of their absence in the other
631 hydrogels, irrespective of particle size (**Figure 8**). It is worth noting that the sensory perception
632 of particles is not only dictated by the particle size, but also by its concentration, shape,
633 roughness and hardness of the particles as well as the properties of the matrix in which it is
634 dispersed. For example, the sensory threshold for particle size in chocolate is $\sim 30 \mu\text{m}$

635 (Afoakwa, Paterson, & Fowler, 2007) whereas for sharp-faceted silica particles it is as low as
636 2 μm (Engelen, et al., 2005) the be perceived as rough and/or gritty. Also, a thicker matrix can
637 mask the sensory detection of particles (Imai, Hatae, & Shimada, 1995; Sala & Scholten, 2015).
638 Thus, the observed low ratings in sensory smoothness might have resulted from these soft big
639 CaA beads ($\geq 300 \mu\text{m}$) with sizes much above the sensory detection threshold, the inability of
640 the κC matrix to mask such perceptions as well as the absence of any ball-bearing effects.

641 It is worth highlighting that although the κC hydrogels scored high on the sensory
642 attribute ‘smooth’ (**Figure 8**), the friction coefficients of κC hydrogel bolus filtrates were
643 highest in the boundary regime ($\mu \sim 0.5$) (**Figure 4b**). Noteworthy is that the PDMS substrates
644 used in this study for tribology were highly hydrophobic (even after pre-adsorption of artificial
645 saliva), which might not have allowed efficient polymer-adsorption of the hydrophilic κC
646 hydrogel bolus particles remaining in the filtrate to the substrates and thus did not reduce
647 friction significantly ($p > 0.05$). This might not be the case during real oral processing as the
648 oral mucosa is highly hydrophilic because of the salivary coating (Laguna & Sarkar, 2017).
649 Hence, one might consider introducing some degree of hydrophilicity in these soft PDMS
650 substrates for doing oral tribology measurements in order to accurately understand this sensory
651 smoothness scores for κC hydrogels (Sarkar, et al., 2017a). Interestingly, the friction
652 coefficients of the κC hydrogel bolus fragments (particularly $3\kappa\text{C}$) was considerably low ($\mu \sim$
653 0.15) in the boundary regime (**Figure 4a, Table 3**). This suggests that the $3\kappa\text{C}$ gel bolus
654 fragments were responsible for acting as a solvated layer of lubricant to reduce viscous friction,
655 as discussed previously, and consequently were rated high on the sensory attribute, ‘smooth’
656 (**Figure 8**).

657 For the attributes ‘slippery’ and ‘salivating’, the trend was not very clear for samples
658 containing NaA or CaA (**Figure 8**), which might be associated with the rather difficult
659 definitions and the unfamiliarity of the panel with these lubrication-related texture attributes.

660 This can also be seen in the Tucker-1 plots, see **Supplementary Figure 2**, where the attributes
661 ‘slippery’ and salivating’ showed rather random clustering patterns indicative of poor panel
662 agreement. It appears that insufficient training was provided to the participants on these
663 constructs for them to grasp the complexity of these attributes in novel semi-solid systems *i.e.*
664 the hydrogels with different textural complexity. Only samples containing NaA scored
665 significantly lower on ‘salivating’ as compared to that of κ C or κ C/LBG hydrogels ($p < 0.05$).
666 ‘Salivating’ was defined as ‘amount of saliva released during chewing’ (**Table 2**). Therefore,
667 it is likely that panellists rated κ C or κ C/LBG hydrogels as more ‘salivating’ compared to that
668 of NaA samples ($p < 0.05$) as possibly a larger quantity of saliva was generated for cleansing
669 the residues of the stiffer hydrogel fragments (**Figure 1**). Similarly, samples containing NaA
670 and CaA (except 1.6 κ C0.2CaA₃₀₀) scored significantly lower on the attribute ‘slippery’
671 compared to that of κ C hydrogels ($p < 0.05$). This suggests that samples containing alginate
672 as biopolymer or beads did not slip easily and provided some sort of oral coating properties
673 due to the alginate itself or created a ‘weeping’ layer of water as a lubricant during tribological
674 shearing (Gong & Osada, 2002), as discussed in the previous section. The oral coating property
675 of alginates is in agreement with literature suggesting that alginate can create hydrogen bonds
676 with human salivary mucins through carboxyl–hydroxyl interactions (Cook, Bull, Methven,
677 Parker, & Khutoryanskiy, 2017; Shtenberg, et al., 2018).

678 In general, it can be concluded that all chewing-related attributes were largely
679 controlled by the fracture properties of the hydrogels, whereas the lubrication-related attributes
680 showed significant variations between the hydrogel samples and some of the lubrication-related
681 attributes corroborated the oral tribology results of the gel bolus filtrates in the mixed
682 lubrication regime. Noteworthy is that the relationship between fracture properties, tribology
683 and sensory analysis has been investigated in literature, particularly in emulsion gels
684 (Devezeaux de Lavergne, van Delft, van de Velde, van Boekel, & Stieger, 2015b; Liu, Stieger,

685 van der Linden, & van de Velde, 2016). Nevertheless, to our knowledge, this is the first study
686 that has been carried out using descriptive sensory analysis focussing on textural attributes
687 related to both chewing and lubrication in aqueous systems *i.e.* hydrogels with varying degree
688 of textural complexity.

689

690 **3.3. Relationship between the and sensory properties of the hydrogels**

691 To understand the complex sensory perceptions in these hydrogels with or without
692 inhomogeneity, an integrative approach of identifying interrelationships between sensory
693 textural attributes and instrumental parameters rather than dependence on a single instrumental
694 test is necessary. **Table 6** highlights the statistically significant correlation coefficients between
695 the broad spectrum of mechanical parameters, *i.e.* fracture properties, apparent viscosity, μ in
696 boundary and mixed lubrication regime, and the texture attributes.

697 Positive correlations were obtained between the chewing-related sensory attributes, *i.e.*,
698 ‘firm’, ‘elastic’, ‘chewy’ and ‘cohesive’ and the instrumental measures of fracture stress,
699 fracture strain, fracture energy and viscosity at 50 s^{-1} (**Table 6**). The correlations of the fracture
700 parameters with the chewing-related attributes are in agreement with previous literature dealing
701 with emulsion gels (Devezeaux de Lavergne, et al., 2015a) and agarose gels (Barrangou, Drake,
702 Daubert, & Foegeding, 2006). This suggests that firm samples, such as κC and $\kappa\text{C/LBG}$ will
703 require more stress to deform, particularly in the early stages of oral processing.

704 Interestingly, the lubrication-related sensory attribute ‘salivating’ also showed strong
705 positive correlations with instrumental measures of fracture stress, fracture strain, fracture
706 energy and viscosity at 50 s^{-1} , respectively. As discussed previously, the firm samples might
707 have created residues/particles, which required increased salivary flow for oral cleansing
708 (**Table 2**). Hence, it appears that the trained panel might have associated sensory ‘salivating’
709 with the quantity rather than the quality of saliva production. In addition, strong inverse

710 relationships were obtained between ‘pasty’, and ‘melting’ and the instrumental measures of
711 fracture stress, fracture strain, fracture energy of the hydrogels and viscosity of boli at 50 s^{-1}
712 ($p < 0.01$). In other words, ‘firm’ samples, such as κC or $\kappa\text{C/LBG}$ hydrogels might have created
713 bolus fragments during the oral processing that were relatively stiff, retained their integrity and
714 were not melting easily over the duration of the oral residence time. In addition, due to such
715 fragment creation, firm samples were not perceived to be ‘pasty’ ($p < 0.01$) *i.e.* did not form a
716 semi-solid continuous layer. Although the sensory attribute ‘smooth’ showed no correlations
717 with either the fracture properties of the hydrogels or the viscosity of the boli, the sensory
718 attribute ‘slippery’ showed a positive correlation with initial fracture stress and fracture strain,
719 which suggests that the term ‘slippery’ had some association with early stages of oral
720 processing, which was not expected ($p > 0.05$). Overall, clear relationships existed between all
721 fracture properties of the hydrogels and rheology of the bolus fragments with lubrication-
722 related attributes, such as ‘pasty’, ‘melting’ and ‘salivating’ that were perceived by the
723 panellists during oral processing.

724 We now shift our focus to investigate whether μ of the hydrogel fragments and/or
725 filtrates could predict the sensory dimensions of both chewing- and lubrication-related texture
726 attributes (**Table 6**). As one might expect, no correlations existed between the chewing-related
727 attributes and μ of bolus fragments/filtrates irrespective of the lubrication regimes. However,
728 looking at the lubrication-related sensory attributes (**Table 6**), ‘pasty’ was inversely correlated
729 with the μ of hydrogel bolus filtrates in the mixed lubrication regimes ($p < 0.05$). This further
730 suggests that ‘pasty’ was most likely associated with the mouth-coating aspects during oral
731 processing, as discussed previously. For example, samples with lower μ values (*e.g.*
732 $1.5\kappa\text{C}0.5\text{NaA}$) in the boundary regime will be more lubricating and will thus be perceived as
733 more ‘pasty’ forming an oral coating and/or ‘weeping’ layer of water, separating the oral
734 surfaces from the asperity contacts. Although the signs of correlations in case of the tribology

735 experiments performed with hydrogel bolus fragments were similar to that of the hydrogel
736 bolus filtrate, no significance was observed in the former irrespective of the lubrication-related
737 attribute. This confirms that the bolus filtrates being thin-film had more relevance in the oral
738 tribology domain in this study when relating to the in-mouth sensory perception as compared
739 to that of the bolus gel fragments.

740 Interestingly, there was a tendency towards an inverse relationship of sensory ‘melting’
741 to the μ of the hydrogel bolus filtrates in the mixed lubrication regime, however there was no
742 statistical significance (**Table 6**). Moreover, ‘salivating’ was positively correlated with the μ
743 of the bolus fragments ($p < 0.05$). This is in agreement with the explanation for the initial
744 fracture properties, which suggests that hydrogels scoring higher on ‘salivating’ were the
745 samples that generated more volume of saliva (**Table 2**). As can be expected, the generated
746 saliva was perhaps depleting the gel fragments or residues from the oral surfaces. Such
747 ‘depletion’ of bolus fragments or residues from the oral surfaces might have resulted in
748 apparent surface asperity contacts, which may justify the positive correlation of ‘salivating’
749 with friction coefficients as observed in **Table 6**. No relationships could be observed between
750 ‘smooth’ and μ of bolus filtrates, which might be attributed to the inhomogeneity of samples,
751 such as the ones containing CaA beads. For the sensory attribute ‘slippery’, there was a positive
752 correlation with μ of hydrogel bolus filtrates in the mixed lubrication regime ($p < 0.05$) (**Table**
753 **6**).

754 It is worth highlighting this observed anomaly when relating the sensory attribute of
755 ‘slippery’ to the tribology results. Previously, an inverse relationship of friction coefficient and
756 slipperiness in foods, *i.e.* $slipperiness \propto \frac{1}{\text{viscous force} + W\mu}$ (where W is the applied load in
757 tribology), has been postulated by Kokini (1987). However, this previous study by Kokini
758 (1987) was done with fat-rich low viscosity fluids, where ‘slipperiness’ could be perceived
759 easily due to ‘fatty’ or ‘creamy mouthfeel’. In comparison, the current study has employed

760 semi-solid aqueous hydrogels and their corresponding bolus fragments and filtrates.
761 Furthermore, ‘slippery’ perception was defined by the ease of sliding of the sample (**Table 2**).
762 This suggests that highly slippery samples, such as 2κC gels (**Figure 8**) were sliding past the
763 oral mucosa easily, which apparently resulted in having no fragments/ filtrate in the
764 confinement, corroborating with the high μ values (**Figure 4b, Table 3**). Nevertheless, it is
765 worth to emphasize that both ‘slippery’ and ‘salivating’ were difficult sensory terms for the
766 panellists (**Figure 8**), as discussed before, and thus these correlations might be taken with some
767 degree of precaution.

768

769 **4. Conclusions**

770 This study presents hydrogels as model semi-solid foods, where systematic
771 manipulation of the structural properties was used to investigate the relationship between
772 mechanical (instrumentally measured) and sensory aspects of oral processing. A range of
773 hydrogels with varying degrees of structural complexity was evaluated using uniaxial
774 compression test of the hydrogels, flow curves and tribology of gel boli (after simulated oral
775 processing) as well the sensory properties, which was investigated using descriptive sensory
776 analysis. Tribology of the bolus fragments and filtrates were explained using theoretical
777 “repulsion-adsorption” model highlighting the role of opposing surfaces (PDMS, gels). A clear
778 correlation was obtained between the initial fracture properties of the hydrogels, viscosity of
779 the bolus fragments and all chewing-related texture attributes i.e. ‘firm’, ‘elastic’, ‘chewy’ and
780 ‘cohesive’. Interestingly, all fracture attributes and boli viscosity showed positive correlation
781 to the relatively novel lubrication-related texture attributes, such as ‘salivating’ and inverse
782 correlations with both ‘pasty’ and ‘melting’. The coefficient of friction of the bolus filtrates in
783 the mixed lubrication regime showed inverse correlations with the lubrication-related
784 attributes, such as sensory ‘pasty’ and positive correlations with ‘slippery’ and ‘salivating’.

785 However, our experimental design could not establish a significant inverse correlation between
786 sensory ‘smooth’ and the friction coefficients, which is largely attributed to the inhomogeneity
787 of the samples employed in the study. Novel findings from this study suggests that lubrication-
788 related attributes were perceived during both early and later stages of oral processing and thus
789 relationships existed with initial fracture properties of gels, boli viscosity and boli tribology
790 and not only to boli tribology, as hypothesized initially. Future studies should focus on further
791 training of panel members particularly with respect to lubrication-related texture attributes. In
792 addition, more independent systematic studies with hydrogels with varying degrees of
793 structural complexity at micro- to macro-scale are needed to clearly establish the tribology-
794 sensory relationships particularly at the later stages of oral processing.

795

796 **Acknowledgements**

797 We thank Siti Ahmad for her help in formulating the preliminary hydrogels, as well as we thank
798 all participants for their time and willingness to taste the model hydrogels. Author (EK)
799 acknowledges University of Leeds 110 Anniversary Research Scholarship with matched
800 support from Mars Wrigley Confectionery for funding her PhD studies.

801

802 **References**

803 Afoakwa, E. O., Paterson, A., & Fowler, M. (2007). Factors influencing rheological and
804 textural qualities in chocolate – a review. *Trends in Food Science & Technology*, 18(6),
805 290-298.

806 Barrangou, L. M., Drake, M., Daubert, C. R., & Foegeding, E. A. (2006). Textural properties
807 of agarose gels. II. Relationships between rheological properties and sensory texture.
808 *Food Hydrocolloids*, 20(2), 196-203.

809 Bongaerts, J. H. H., Cooper-White, J. J., & Stokes, J. R. (2009). Low biofouling chitosan-
810 hyaluronic acid multilayers with ultra-low friction coefficients. *Biomacromolecules*,
811 *10*(5), 1287-1294.

812 Bongaerts, J. H. H., Fourtouni, K., & Stokes, J. R. (2007a). Soft-tribology: Lubrication in a
813 compliant PDMS–PDMS contact. *Tribology International*, *40*(10–12), 1531-1542.

814 Bongaerts, J. H. H., Rossetti, D., & Stokes, J. R. (2007b). The lubricating properties of human
815 whole saliva. *Tribology letters*, *27*(3), 277-287.

816 Chen, J., & Stokes, J. R. (2012). Rheology and tribology: Two distinctive regimes of food
817 texture sensation. *Trends in Food Science & Technology*, *25*(1), 4-12.

818 Cook, S. L., Bull, S. P., Methven, L., Parker, J. K., & Khutoryanskiy, V. V. (2017).
819 Mucoadhesion: A food perspective. *Food Hydrocolloids*, *72*, 281-296.

820 Czaczyk, K., Olejnik, A., & Trojanowska, K. (1999). The influence of LBG addition to
821 carrageenan on the mechanical stability of the gel and the fermentative activity of
822 immobilized propionic acid bacteria. *Acta Biotechnologica*, *19*(2), 147-156.

823 de Vicente, J., Stokes, J. R., & Spikes, H. A. (2005). The Frictional Properties of Newtonian
824 Fluids in Rolling–Sliding soft-EHL Contact. *Tribology Letters*, *20*(3), 273-286.

825 Dea, I. C. M., & Morrison, A. (1975). Chemistry and Interactions of Seed Galactomannans. In
826 R. S. Tipson & D. Horton (Eds.), *Advances in Carbohydrate Chemistry and*
827 *Biochemistry* (Vol. 31, pp. 241-312): Academic Press.

828 Devezeaux de Lavergne, M., Strijbosch, V. M. G., Van den Broek, A. W. M., Van de Velde,
829 F., & Stieger, M. (2016). Uncoupling the Impact of Fracture Properties and
830 Composition on Sensory Perception of Emulsion-Filled Gels. *Journal of Texture*
831 *Studies*, *47*(2), 92-111.

832 Devezeaux de Lavergne, M., van de Velde, F., van Boekel, M. A. J. S., & Stieger, M. (2015a).
833 Dynamic texture perception and oral processing of semi-solid food gels: Part 2: Impact
834 of breakdown behaviour on bolus properties and dynamic texture perception. *Food*
835 *Hydrocolloids*, 49, 61-72.

836 Devezeaux de Lavergne, M., van Delft, M., van de Velde, F., van Boekel, M. A. J. S., & Stieger,
837 M. (2015b). Dynamic texture perception and oral processing of semi-solid food gels:
838 Part 1: Comparison between QDA, progressive profiling and TDS. *Food*
839 *Hydrocolloids*, 43, 207-217.

840 Dunstan, D. E., Chen, Y., Liao, M. L., Salvatore, R., Boger, D. V., & Prica, M. (2001).
841 Structure and rheology of the κ -carrageenan/locust bean gum gels. *Food Hydrocolloids*,
842 15(4-6), 475-484.

843 Engelen, L., de Wijk, R. A., van der Bilt, A., Prinz, J. F., Janssen, A. M., & Bosman, F. (2005).
844 Relating particles and texture perception. *Physiology & Behavior*, 86(1), 111-117.

845 Field, A. (2017). *Discovering statistics using IBM SPSS statistics* London, United Kingdom:
846 Sage Publications Ltd.

847 Foegeding, E. A., Daubert, C. R., Drake, M. A., Essick, G., Trulsson, M., Vinyard, C. J., &
848 Van De Velde, F. (2011). A comprehensive approach to understanding textural
849 properties of semi- and soft-solid foods. *Journal of Texture Studies*, 42(2), 103-129.

850 Funami, T., Ishihara, S., Nakauma, M., Kohyama, K., & Nishinari, K. (2012). Texture design
851 for products using food hydrocolloids. *Food Hydrocolloids*, 26(2), 412-420.

852 Garrec, D. A., & Norton, I. T. (2013). Kappa carrageenan fluid gel material properties. Part 2:
853 Tribology. *Food Hydrocolloids*, 33(1), 160-167.

854 Goh, K. K. T., Sarkar, A., & Singh, H. (2008). Chapter 12 - Milk protein-polysaccharide
855 interactions. In *Milk Proteins* (pp. 347-376). San Diego: Academic Press.

- 856 Goh, K. K. T., Sarkar, A., & Singh, H. (2014). Chapter 13 - Milk Protein–Polysaccharide
857 Interactions. In *Milk Proteins (Second edition)* (pp. 387-419). San Diego: Academic
858 Press.
- 859 Gong, J., & Osada, Y. (1998). Gel friction: A model based on surface repulsion and adsorption.
860 *The Journal of Chemical Physics*, *109*(18), 8062-8068.
- 861 Gong, J. P. (2006). Friction and lubrication of hydrogels-its richness and complexity. *Soft*
862 *Matter*, *2*(7), 544-552.
- 863 Gong, J. P., Kagata, G., Iwasaki, Y., & Osada, Y. (2001). Surface friction of polymer gels: 1.
864 Effect of interfacial interaction. *Wear*, *251*(1), 1183-1187.
- 865 Gong, J. P., Kagata, G., & Osada, Y. (1999). Friction of gels. 4. Friction on charged gels. *The*
866 *Journal of Physical Chemistry B*, *103*(29), 6007-6014.
- 867 Gong, J. P., & Osada, Y. (2002). Surface friction of polymer gels. *Progress in Polymer Science*,
868 *27*(1), 3-38.
- 869 Hayakawa, F., Kazami, Y., Ishihara, S., Nakao, S., Nakauma, M., Funami, T., Nishinari, K., &
870 Kohyama, K. (2014). Characterization of eating difficulty by sensory evaluation of
871 hydrocolloid gels. *Food Hydrocolloids*, *38*, 95-103.
- 872 Hori, K., Hayashi, H., Yokoyama, S., Ono, T., Ishihara, S., Magara, J., Taniguchi, H., Funami,
873 T., Maeda, Y., & Inoue, M. (2015). Comparison of mechanical analyses and tongue
874 pressure analyses during squeezing and swallowing of gels. *Food Hydrocolloids*, *44*,
875 145-155.
- 876 Hutchings, J. B., & Lillford, P. J. (1988). The perception of food texture - the philosophy of
877 the breakdown path. *Journal of Texture Studies*, *19*(2), 103-115.

878 Imai, E., Hatae, K., & Shimada, A. (1995). Oral perception of grittiness: Effect of particle size
879 and concentration of the dispersed particles and the dispersion medium. *Journal of*
880 *Texture Studies*, 26(5), 561-576.

881 Ishihara, S., Nakauma, M., Funami, T., Odake, S., & Nishinari, K. (2011). Viscoelastic and
882 fragmentation characters of model bolus from polysaccharide gels after instrumental
883 mastication. *Food Hydrocolloids*, 25(5), 1210-1218.

884 Johnson, K. L. (2009). Normal Contact Of Elastic Solids: Hertz Theory. In *Contact Mechanics:*
885 Cambridge University Press.

886 Johnston, I. D., McCluskey, D. K., Tan, C. K. L., & Tracey, M. C. (2014). Mechanical
887 characterization of bulk Sylgard 184 for microfluidics and microengineering. *Journal*
888 *of Micromechanics and Microengineering*, 24(3).

889 Kohyama, K., Hayakawa, F., Kazami, Y., Ishihara, S., Nakao, S., Funami, T., & Nishinari, K.
890 (2015). Electromyographic texture characterization of hydrocolloid gels as model foods
891 with varying mastication and swallowing difficulties. *Food Hydrocolloids*, 43, 146-
892 152.

893 Kokini, J. L. (1987). The physical basis of liquid food texture and texture-taste interactions.
894 *Journal of Food Engineering*, 6(1), 51-81.

895 Krop, E. M., Hetherington, M. M., Nekitsing, C., Miquel, S., Postelnicu, L., & Sarkar, A.
896 (2018). Influence of oral processing on appetite and food intake – A systematic review
897 and meta-analysis. *Appetite*, 125, 253-269.

898 Laguna, L., Farrell, G., Bryant, M., Morina, A., & Sarkar, A. (2017a). Relating rheology and
899 tribology of commercial dairy colloids to sensory perception. *Food & Function*, 8(2),
900 563-573.

- 901 Laguna, L., Hetherington, M. M., Chen, J., Artigas, G., & Sarkar, A. (2016). Measuring eating
902 capability, liking and difficulty perception of older adults: A textural consideration.
903 *Food Quality and Preference*, *53*, 47-56.
- 904 Laguna, L., & Sarkar, A. (2016). Influence of mixed gel structuring with different degrees of
905 matrix inhomogeneity on oral residence time. *Food Hydrocolloids*, *61*, 286-299.
- 906 Laguna, L., & Sarkar, A. (2017). Oral tribology: update on the relevance to study astringency
907 in wines. *Tribology - Materials, Surfaces & Interfaces*, *11*(2), 116-123.
- 908 Laguna, L., Sarkar, A., Bryant, M. G., Beadling, A. R., Bartolomé, B., & Victoria Moreno-
909 Arribas, M. (2017b). Exploring mouthfeel in model wines: Sensory-to-instrumental
910 approaches. *Food Research International*, *102*, 478-486.
- 911 Larsen, B. E., Bjørnstad, J., Pettersen, E. O., Tønnesen, H. H., & Melvik, J. E. (2015).
912 Rheological characterization of an injectable alginate gel system. *BMC Biotechnology*,
913 *15*, 29.
- 914 Liu, K., Stieger, M., van der Linden, E., & van de Velde, F. (2016). Effect of microparticulated
915 whey protein on sensory properties of liquid and semi-solid model foods. *Food*
916 *Hydrocolloids*, *60*, 186-198.
- 917 Liu, K., Tian, Y., Stieger, M., van der Linden, E., & van de Velde, F. (2016). Evidence for ball-
918 bearing mechanism of microparticulated whey protein as fat replacer in liquid and semi-
919 solid multi-component model foods. *Food Hydrocolloids*, *52*, 403-414.
- 920 Madsen, J. B., Sotres, J., Pakkanen, K. I., Efler, P., Svensson, B., Abou Hachem, M.,
921 Arnebrant, T., & Lee, S. (2016). Structural and mechanical properties of thin films of
922 bovine submaxillary mucin versus porcine gastric mucin on a hydrophobic surface in
923 aqueous solutions. *Langmuir*, *32*(38), 9687-9696.

924 Minekus, M., Alming, M., Alvito, P., Ballance, S., Bohn, T., Bourlieu, C., Carriere, F.,
925 Boutrou, R., Corredig, M., Dupont, D., Dufour, C., Egger, L., Golding, M., Karakaya,
926 S., Kirkhus, B., Le Feunteun, S., Lesmes, U., Macierzanka, A., Mackie, A., Marze, S.,
927 McClements, D. J., Menard, O., Recio, I., Santos, C. N., Singh, R. P., Vegarud, G. E.,
928 Wickham, M. S. J., Weitschies, W., & Brodkorb, A. (2014). A standardised static in
929 vitro digestion method suitable for food - an international consensus. *Food & Function*,
930 5(6), 1113-1124.

931 Miquel-Kergoat, S., Azais-Braesco, V., Burton-Freeman, B., & Hetherington, M. M. (2015).
932 Effects of chewing on appetite, food intake and gut hormones: A systematic review and
933 meta-analysis. *Physiology & Behavior*, 151, 88-96.

934 Morell, P., Chen, J., & Fiszman, S. (2017). The role of starch and saliva in tribology studies
935 and the sensory perception of protein-added yogurts. *Food & Function*, 8(2), 545-553.

936 Peleg, M. (1984). A note on the various strain measures at large compressive deformations.
937 *Journal of Texture Studies*, 15(4), 317-326.

938 Pradal, C., & Stokes, J. R. (2016). Oral tribology: bridging the gap between physical
939 measurements and sensory experience. *Current Opinion in Food Science*, 9, 34-41.

940 Prakash, S., Tan, D. D. Y., & Chen, J. (2013). Applications of tribology in studying food oral
941 processing and texture perception. *Food Research International*, 54(2), 1627-1635.

942 Puttock, M. J., & Thwaite, E. G. (1969). Elastic Compression of Spheres and Cylinders at Point
943 and Line Contact. *National Standards Laboratory Technical Paper*, 25.

944 Sala, G., & Scholten, E. (2015). Chapter 5 - Instrumental characterisation of textural properties
945 of fluid food A2 - Chen, Jianshe. In A. Rosenthal (Ed.), *Modifying Food Texture* (pp.
946 107-131): Woodhead Publishing.

- 947 Santagiuliana, M., Piqueras-Fiszman, B., van der Linden, E., Stieger, M., & Scholten, E.
948 (2018). Mechanical properties affect detectability of perceived texture contrast in
949 heterogeneous food gels. *Food Hydrocolloids*, 80, 254-263.
- 950 Sarkar, A., Goh, K. K. T., & Singh, H. (2009). Colloidal stability and interactions of milk-
951 protein-stabilized emulsions in an artificial saliva. *Food Hydrocolloids*, 23(5), 1270-
952 1278.
- 953 Sarkar, A., Kanti, F., Gulotta, A., Murray, B. S., & Zhang, S. (2017a). Aqueous lubrication,
954 structure and rheological properties of whey protein microgel particles. *Langmuir*,
955 33(51), 14699-14708.
- 956 Sarkar, A., & Singh, H. (2012). Oral behaviour of food emulsions. In *Food Oral Processing*
957 (pp. 111-137): Wiley-Blackwell.
- 958 Sarkar, A., Ye, A., & Singh, H. (2017b). Oral processing of emulsion systems from a colloidal
959 perspective. *Food & Function*, 8(2), 511-521.
- 960 Schipper, R. G., Silletti, E., & Vingerhoeds, M. H. (2007). Saliva as research material:
961 biochemical, physicochemical and practical aspects. *Arch Oral Biol*, 52(12), 1114-
962 1135.
- 963 Shtenberg, Y., Goldfeder, M., Prinz, H., Shainsky, J., Ghantous, Y., Abu El-Naaj, I., Schroeder,
964 A., & Bianco-Peled, H. (2018). Mucoadhesive alginate pastes with embedded
965 liposomes for local oral drug delivery. *International Journal of Biological*
966 *Macromolecules*, 111, 62-69.
- 967 Stading, M., & Hermansson, A.-M. (1993). Rheological behaviour of mixed gels of κ -
968 carrageenan-locust bean gum. *Carbohydrate Polymers*, 22(1), 49-56.
- 969 Steele, C. M., & Van Lieshout, P. (2009). Tongue movements during water swallowing in
970 healthy young and older adults. *J Speech Lang Hear Res*, 52(5), 1255-1267.

- 971 Stokes, J. R., Boehm, M. W., & Baier, S. K. (2013). Oral processing, texture and mouthfeel:
972 From rheology to tribology and beyond. *Current Opinion in Colloid & Interface*
973 *Science*, 18(4), 349-359.
- 974 Stokes, J. R., Macakova, L., Chojnicka-Paszun, A., de Kruif, C. G., & de Jongh, H. H. J. (2011).
975 Lubrication, adsorption, and rheology of aqueous polysaccharide solutions. *Langmuir*,
976 27(7), 3474-3484.
- 977 Tang, J., Larsen, D. S., Ferguson, L. R., & James, B. J. (2016). The effect of textural complexity
978 of solid foods on satiation. *Physiology & Behavior*, 163, 17-24.
- 979 Tomic, O., Luciano, G., Nilsen, A., Hyldig, G., Lorensen, K., & Næs, T. (2010). Analysing
980 sensory panel performance in a proficiency test using the PanelCheck software.
981 *European Food Research and Technology*, 230, 497-511.
- 982 van Stee, M.-A., de Hoog, E., & van de Velde, F. (2017). Oral Parameters Affecting Ex-vivo
983 Tribology. *Biotribology*, 11, 84-91.
- 984 Vijay, A., Inui, T., Dodds, M., Proctor, G., & Carpenter, G. (2015). Factors that influence the
985 extensional rheological property of saliva. *PLOS ONE*, 10(8), e0135792.
- 986 Yakubov, G. E., McColl, J., Bongaerts, J. H. H., & Ramsden, J. J. (2009). Viscous boundary
987 lubrication of hydrophobic surfaces by mucin. *Langmuir*, 25(4), 2313-2321.
- 988

Figure 1.

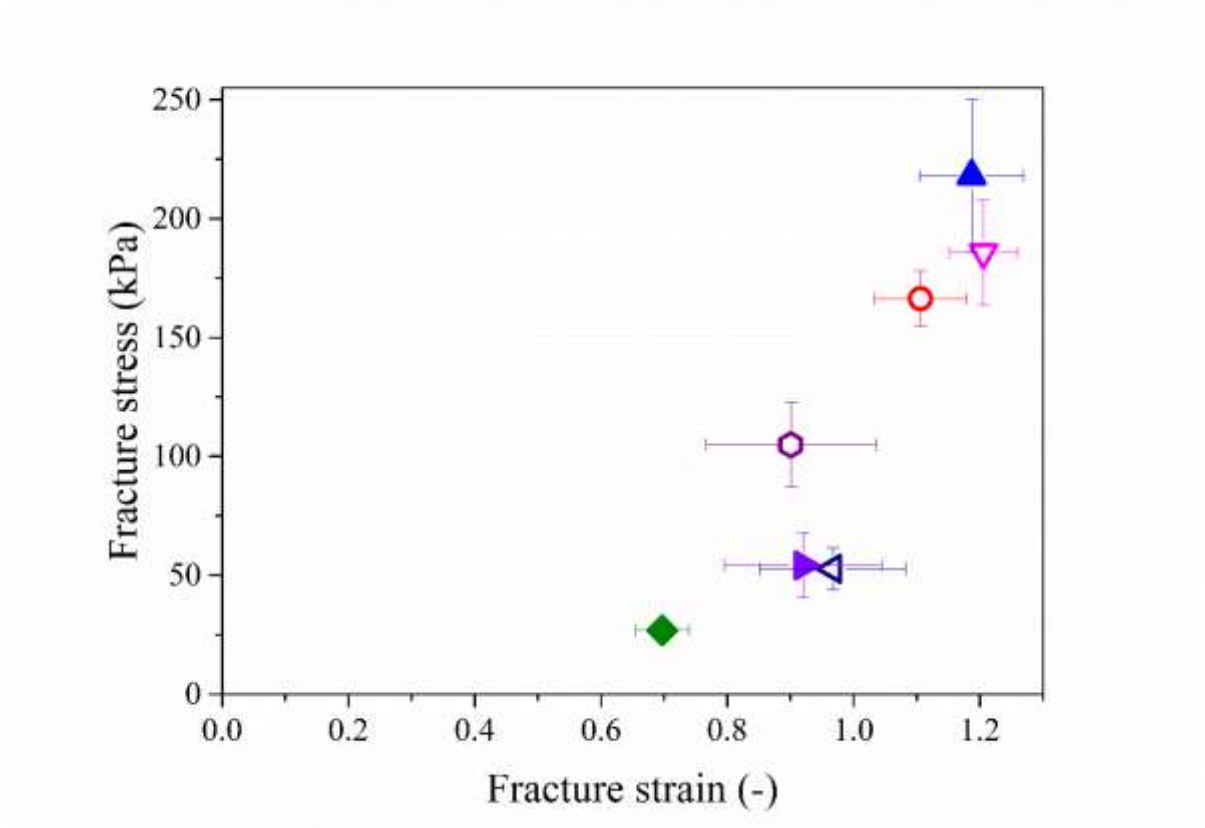


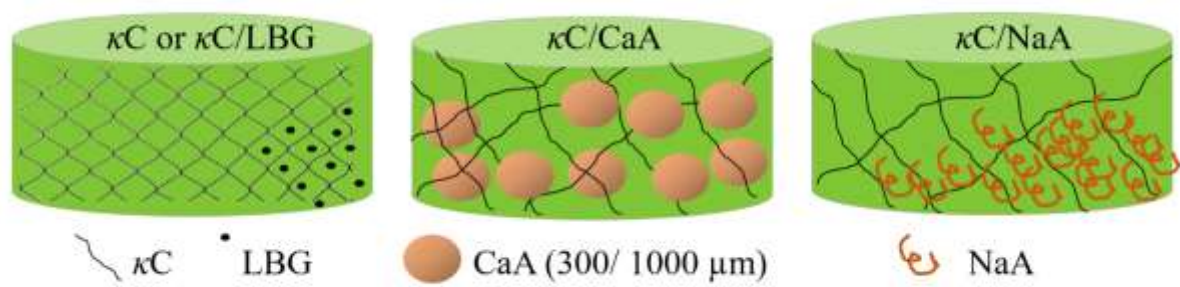
Figure 2.

Figure 3.

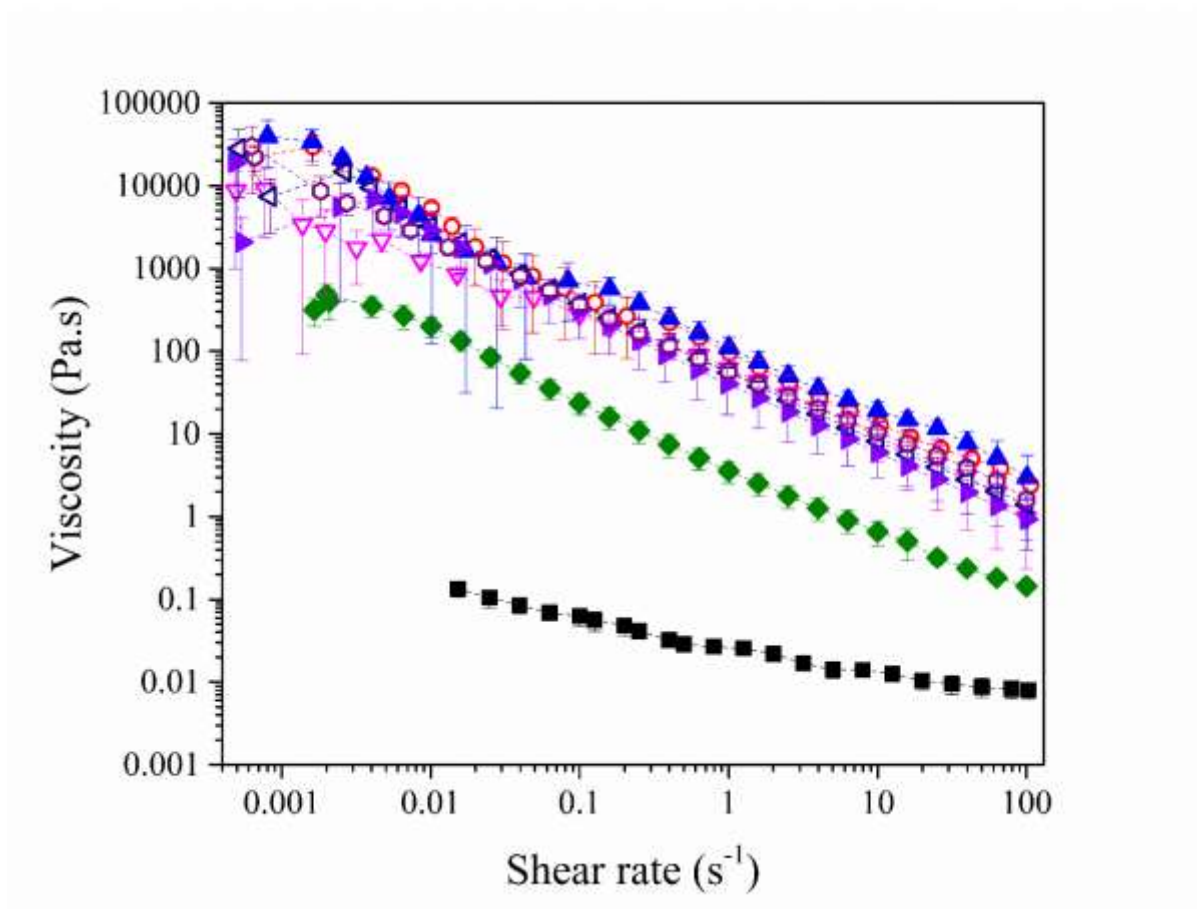


Figure 4.

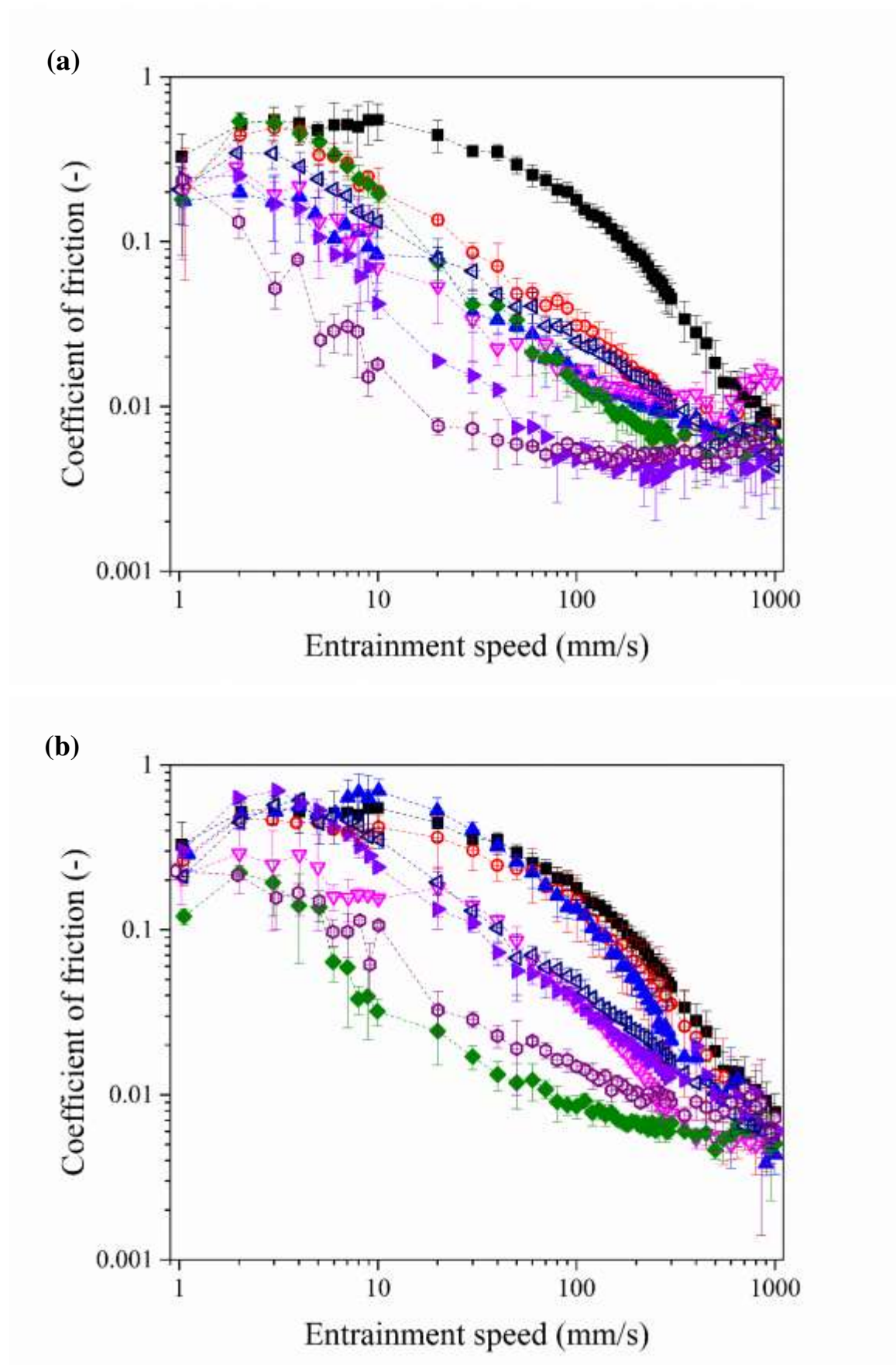


Figure 5.

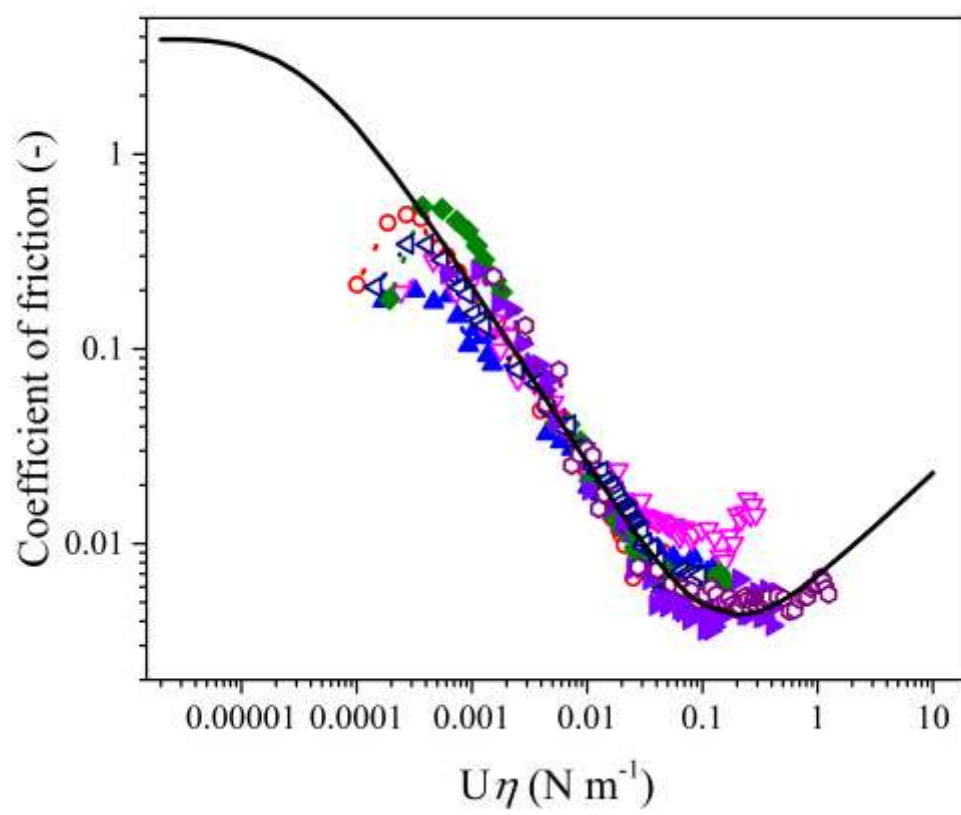


Figure 6.

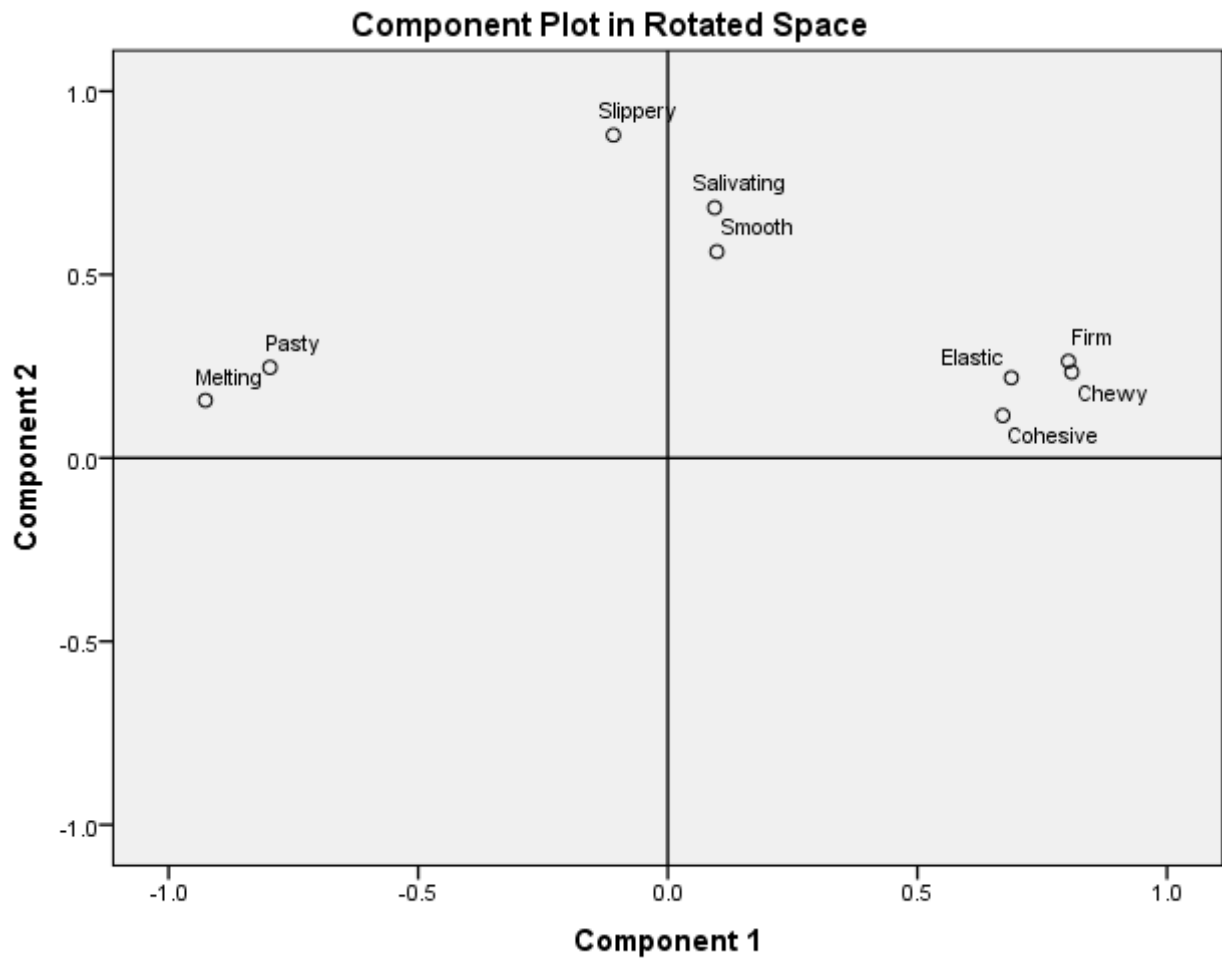


Figure 7.

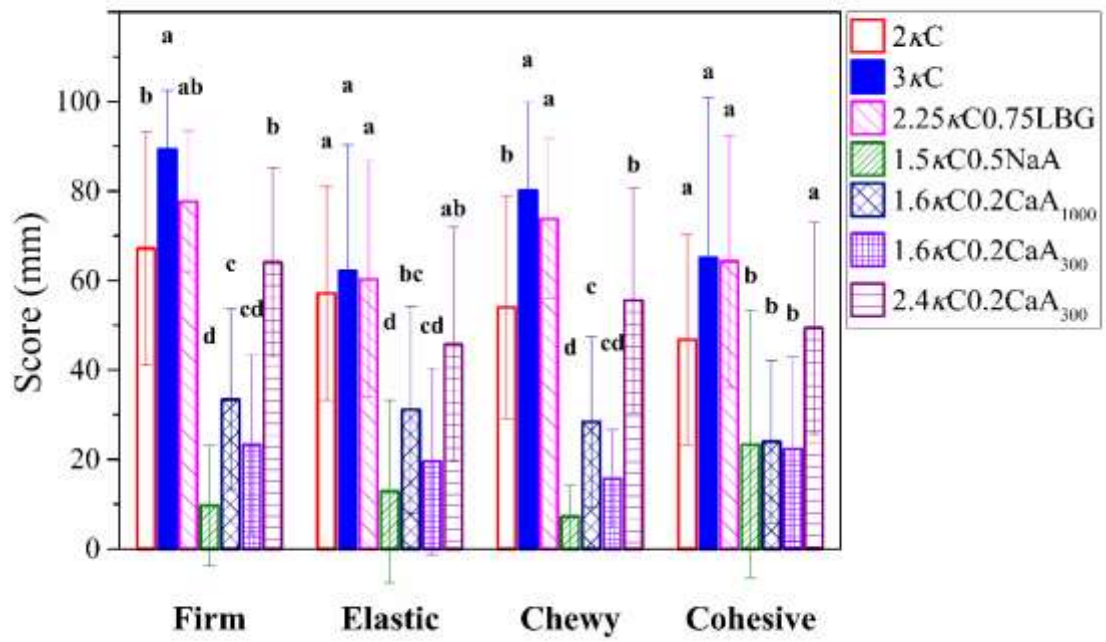
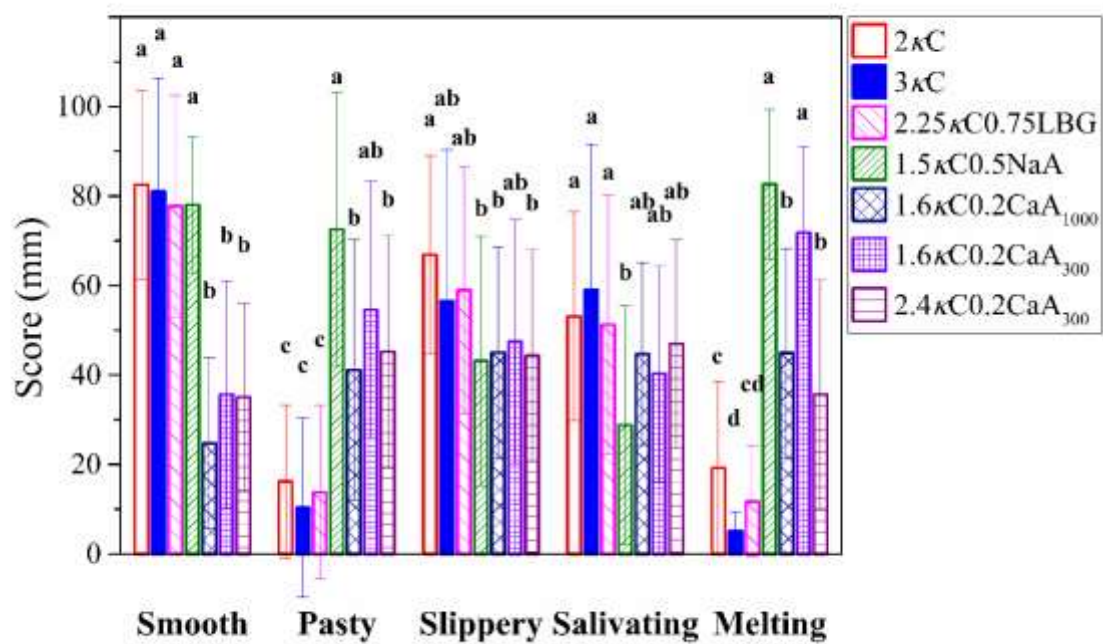


Figure 8.



Captions for Figures

Figure 1. Fracture stress and strain of 2κC (○), 3κC (▲), 2.25κC0.75LBG (▽), 1.5κC0.5NaA (◆), 1.6κC0.2CaA₁₀₀₀ (◁), 1.6κC0.2CaA₃₀₀ (▶) and 2.4κC0.2CaA₃₀₀ (⊙) hydrogels in uniaxial compression test. Data points represent the average of at least three measurements on four different preparation days. Error bars indicate the standard deviation.

Figure 2. Schematic representation of the hydrogels.

Figure 3. Flow curves of artificial saliva (■), 2κC (○), 3κC (▲), 2.25κC0.75LBG (▽), 1.5κC0.5NaA (◆), 1.6κC0.2CaA₁₀₀₀ (◁), 1.6κC0.2CaA₃₀₀ (▶) and 2.4κC0.2CaA₃₀₀ (⊙) gel bolus fragments as a function of shear rate at 37 °C. Data points represent the average of at least three measurements. Error bars indicate the standard deviation.

Figure 4. Friction coefficients of 2κC (○), 3κC (▲), 2.25κC0.75LBG (▽), 1.5κC0.5NaA (◆), 1.6κC0.2CaA₁₀₀₀ (◁), 1.6κC0.2CaA₃₀₀ (▶) and 2.4κC0.2CaA₃₀₀ (⊙) gel bolus fragments (a) and gel bolus filtrates (after filtering out the larger fragments) (b), respectively, after simulated oral processing in presence artificial saliva (■), at 37 °C as a function of entrainment speed. Data points represent the average of at least three measurements. Error bars indicate the standard deviation.

Figure 5. Stribeck master curve for 2κC (○), 3κC (▲), 2.25κC0.75LBG (▽), 1.5κC0.5NaA (◆), 1.6κC0.2CaA₁₀₀₀ (◁), 1.6κC0.2CaA₃₀₀ (▶) and 2.4κC0.2CaA₃₀₀ (⊙) gel bolus fragments as

a function of the product of viscosity and entrainment speed component ($U\eta$). The black solid line is the best fit to the data using Eq (13)

Figure 6. Principal component analysis (PCA) of all texture attributes obtained in the descriptive sensory analysis. Principal component 1 (PC1) represents 48.5% and PC2 15.6% of the variance in the data.

Figure 7. The ratings of the chewing-related attributes obtained from QDA profiling of the gels. Data points represent the average of the gels evaluated in triplicate by 11 panelists. Error bars indicate the standard deviation and bars within one attribute with different lower case letters denote a statistically significant difference ($p < 0.05$).

Figure 8. The ratings of the lubrication-related attributes obtained from QDA profiling of the gels. Data points represent the average of the gels evaluated in triplicate by 11 panelists. Error bars indicate the standard deviation and bars within one attribute with different lower case letters denote a statistically significant difference ($p < 0.05$).

Table 1.

Hydrogel samples	κ -carrageenan (wt%)	Locust bean gum (wt%)	Na-alginate (wt%)	Ca-alginate beads (wt%)	Water (wt%)
2 κ C	2				97
3 κ C	3				96
2.25 κ C0.75LBG	2.25	0.75			96
1.5 κ C0.5NaA	1.5		0.5		97
1.6 κ C0.2CaA ₁₀₀₀	1.6			0.2	97
1.6 κ C0.2CaA ₃₀₀	1.6			0.2	97
2.4 κ C0.2CaA ₃₀₀	2.4			0.2	96

* All hydrogels contained 0.5 wt% green food colouring and 0.5 wt% peppermint flavouring. The two κ -carrageenan hydrogels contained 0.145 wt% KCl. The composition of the mixed hydrogels containing Ca-alginate beads was determined based on the ratio between κ -carrageenan gel matrix (2 or 3 wt%) and Ca-alginate beads (1 wt%), irrespective of bead size.

Table 2.

Textural attributes from QDA profiling	Definition
Smooth	Degree of abrasiveness of the products surface as perceived by the tongue
Firm	The force needed to compress the sample between tongue and palate (hardness)
Elastic	The ease in which the sample bounces back after chewing (springiness)/force with which the sample returns to its original shape after partial compression (without fracture) between the tongue and palate
Chewy	The amount of chews needed to break down the sample to be ready for swallowing
Cohesiveness	Degree to which the samples deforms/holds together rather than crumbles/breaks/ruptures (it conforms to the palate rather than shears)
Pasty	The sensation of the presence of wet/soft (immiscible) solids in the mouth (muddy)
Slippery	The ease in which the sample slides through the mouth during chewing (slimy)
Salivating	The amount of saliva released during chewing
Melting	The amount of sample that dissolves/disappears over time (loss of structure in the mouth) rather than cracking or breaking apart

Table 3.

Samples	Friction force of the gel bolus fragments (N)				Friction force of the gel bolus filtrate (N)			
	Boundary lubrication regime (3 mm/s)		Mixed lubrication regime (50 mm/s)		Boundary lubrication regime (3 mm/s)		Mixed lubrication regime (50 mm/s)	
	Mean	SD	Mean	SD	Mean	SD	Mean	SD
Artificial saliva	1.097 ^a	0.211	0.585 ^a	0.071	1.097 ^a	0.211	0.585 ^a	0.071
2κC	0.978 ^{ab}	0.179	0.096 ^b	0.024	0.928 ^{ab}	0.067	0.469 ^a	0.069
3κC	0.348 ^{cd}	0.146	0.061 ^b	0.010	1.042 ^a	0.047	0.515 ^a	0.059
2.25κC0.75LBG	0.387 ^{cd}	0.076	0.049 ^b	0.018	0.498 ^{bc}	0.301	0.172 ^b	0.036
1.5κC0.5NaA	1.046 ^{ab}	0.125	0.067 ^b	0.011	0.386 ^c	0.143	0.024 ^b	0.007
1.6κC0.2CaA ₁₀₀₀	0.687 ^{bc}	0.135	0.080 ^b	0.017	1.141 ^a	0.103	0.135 ^b	0.055
1.6κC0.2CaA ₃₀₀	0.338 ^{cd}	0.168	0.015 ^b	0.002	1.393 ^a	0.003	0.113 ^b	0.039
2.4κC0.2CaA ₃₀₀	0.104 ^d	0.026	0.012 ^b	0.003	0.313 ^c	0.112	0.038 ^b	0.018

Table 4.

Samples	N_{particle}	F_{particle} (N)	α (mm)
1.6κC0.2CaA1000	0.5	3.90	18.3
1.6κC0.2CaA300	5.7	0.35	5.5
2.4κC0.2CaA300	5.7	0.35	5.5

Table 5.

	PC 1	PC 2
Smooth	.098	.562
Firm	.803	.264
Elastic	.688	.219
Chewy	.809	.234
Cohesive	.671	.116
Pasty	-.797	.247
Slippery	-.109	.880
Salivating	.094	.682
Melting	-.926	.157

Table 6.

		Smooth	Firm	Elastic	Chewy	Cohesive	Pasty	Slippery	Salivating	Melting	Fracture stress	Fracture strain	Fracture Energy	Viscosity at 50 s ⁻¹ shear rate	μ at 50 mm/s	μ at 3 mm/s	μ at 50 mm/s	μ at 3 mm/s
Sensory	Smooth																	
	Firm	0.40																
	Elastic	0.44	0.98															
	Chewy	0.41	0.99	0.98														
	Cohesive	0.53	0.96	0.94	0.98													
	Pasty	-0.43	-0.92	-0.95	-0.91	-0.84												
	Slippery	0.66	0.68	0.77	0.64	0.63	-0.84											
	Salivating	0.25	0.94	0.94	0.91	0.82	-0.95	0.71										
	Melting	-0.38	-0.97	-0.99	-0.97	-0.91	0.97	-0.73	-0.96									
Texture analysis	Fracture stress	0.59	0.96	0.96	0.95	0.95	-0.94	0.80	0.91	-0.94								
	Fracture strain	0.36	0.87	0.90	0.87	0.80	-0.98	0.80	0.92	-0.92	0.91							
	Fracture Energy	0.55	0.89	0.87	0.87	0.84	-0.88	0.72	0.90	-0.87	0.94	0.82						
Rheology	Viscosity at 50 s ⁻¹ shear rate	0.30	0.91	0.89	0.88	0.80	-0.90	0.67	0.98	-0.91	0.80	0.86	0.95					
Tribology, gel bolus filtrate	μ at 50 mm/s	0.56	0.68	0.71	0.63	0.57	-0.80	0.82	0.79	-0.72	0.79	0.74	0.90	0.85				
	μ at 3 mm/s	-0.30	-0.11	-0.11	-0.16	-0.30	-0.15	0.14	0.22	0.04	-0.03	0.25	0.14	0.24	0.39			
Tribology, gel bolus fragments	μ at 50 mm/s	0.47	0.06	0.19	0.05	0.00	-0.31	0.48	0.16	-0.24	0.18	0.22	0.25	0.16	0.56	0.15		
	μ at 3 mm/s	0.42	-0.44	-0.31	-0.45	-0.42	0.22	0.17	-0.40	0.31	-0.28	-0.30	-0.23	-0.37	0.18	0.34	0.81	

Captions for Tables

Table 1. Final composition of the hydrogels.

Table 2. List of attributes and descriptions as included in the QDA profiling.

Table 3. Friction force (N) for the gel bolus fluid (thin liquid) after filtering out the larger fragments at 3 mm/s (boundary lubrication regime) and 50 mm/s (mixed lubrication regime) entrainment speed and 37 °C. The samples were prepared using simulated oral processing in the presence of artificial saliva, and compared to artificial saliva as a control measure. A different lower case letter denotes a statistically significant difference ($p < 0.05$).

Table 4. Elastic compression of the CaA beads based on 10% particle entrainment.

Table 5. Pattern matrix from the Principal Component Analysis (PCA). The Oblimin with Kaiser Normalisation rotation method was applied and the rotation converged in 5 iterations. Highlighted in red shows the sensory attributes best represented in PC1 and PC2 (> 0.500).

Table 6. Pearson's correlations of sensory attributes (QDA) and physical properties (large deformation rheology, apparent viscosity and coefficient of friction) of the hydrogels, where green is positive and red shows a negative correlation with $p < 0.05$ in light colours and $p < 0.01$ in the darker shade.

On relating rheology and oral tribology to sensory properties in hydrogels

Emma M. Krop^a, Marion M. Hetherington^b, Melvin Holmes^a, Sophie Miquel^c, Anwesha Sarkar^{a}*

^a Food Colloids and Processing Group, School of Food Science and Nutrition, University of Leeds, Leeds LS2 9JT, United Kingdom

^b School of Psychology, University of Leeds, Leeds LS2 9JT, United Kingdom

^c Mars Wrigley Confectionery, 1132 West Blackhawk Street, Chicago, IL 60642, USA

*Corresponding author:

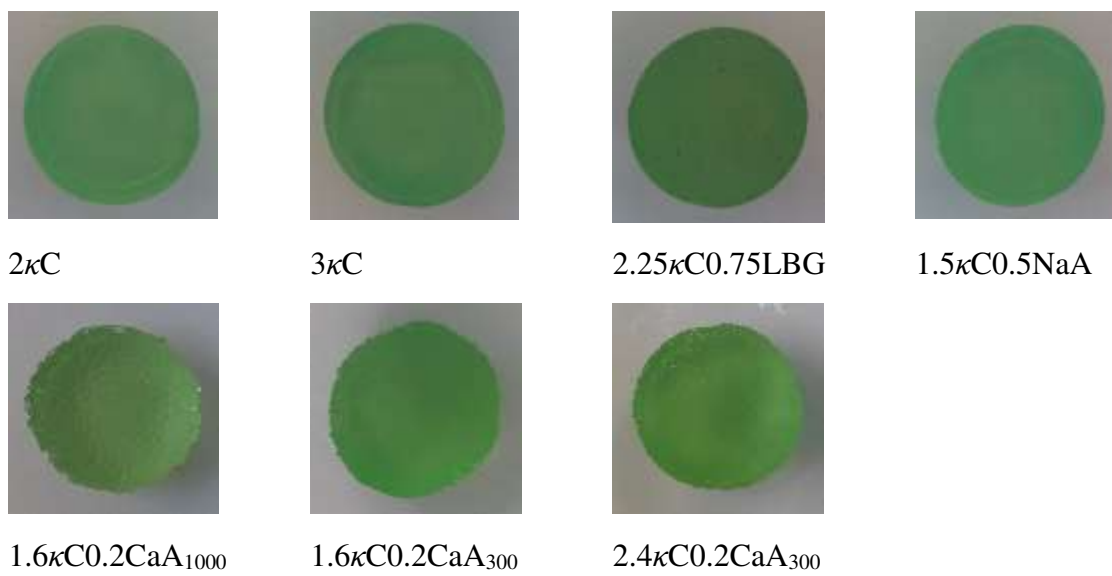
Dr Anwesha Sarkar

Food Colloids and Processing Group,

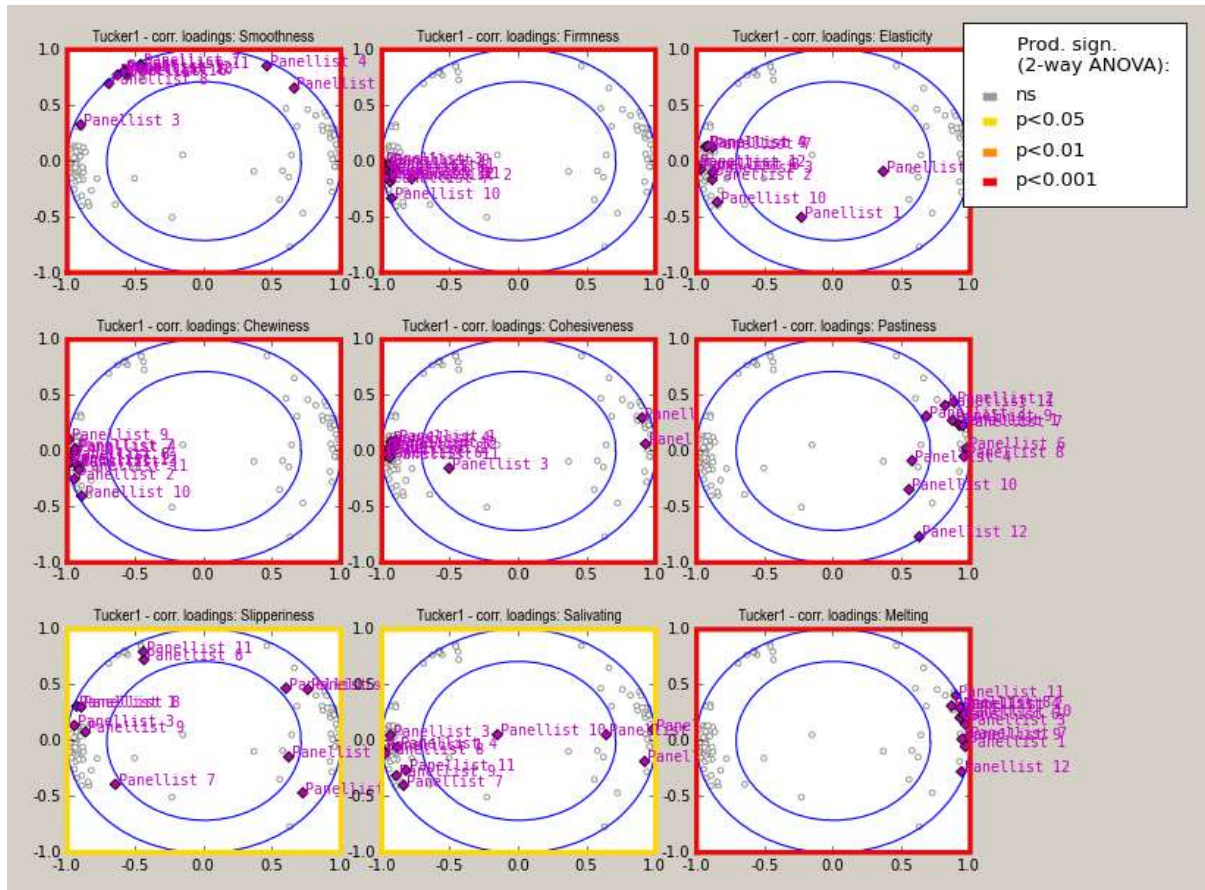
School of Food Science and Nutrition, University of Leeds, Leeds LS2 9JT, UK

E-mail address: A.Sarkar@leeds.ac.uk

Phone: +44 (0) 113 343 2748



Supplementary Figure 1. Visual images of the different hydrogels.



Supplementary Figure 2. Tucker-1 plots for the all attributes from the descriptive sensory analysis, showing the panel agreement.

Supplementary Table 1. Textural properties of the hydrogels obtained from uniaxial compression test. A different lower case letter denotes a statistically significant difference ($p < 0.05$).

Samples	Fracture energy (kPa)	
	Mean	SD
2κC	91.52 ^b	8.31
3κC	147.87 ^a	17.75
2.25κC0.75LBG	71.13 ^c	43.74
1.5κC0.5NaA	6.54 ^f	0.98
1.6κC0.2CaA ₁₀₀₀	26.60 ^e	5.11
1.6κC0.2CaA ₃₀₀	22.39 ^{ef}	7.03
2.4κC0.2CaA ₃₀₀	47.27 ^d	12.85